2018

Development, manufacture and application of a solid-state pH sensor using ruthenium oxide

Wade Lonsdale
Edith Cowan University

Edith Cowan University

Copyright Warning

Development, Manufacture and Application of a Solid-State pH Sensor using Ruthenium Oxide

Wade Lonsdale BSc(Hons)

A thesis submitted in fulfilment of the requirement for the degree of

Doctor of Philosophy

School of Science

Edith Cowan University

Principal Supervisor: Prof. Kamal Alameh

Associate Supervisor: Dr. Magdalena Wajrak

February 2018

Declaration

I certify that this thesis does not, to the best of my knowledge and belief:

I. incorporate without acknowledgement any material previously submitted for a degree or diploma in any institution of higher education;
II. contain any material previously published or written by another person except where due reference is made in the text; or
III. contain any defamatory material
IV. I also grant permission for the Library at Edith Cowan University to make duplicate copies of my thesis as required.

Signature:

Date: 8/6/18

Acknowledgements

I would like to thank my supervisors, Prof. Kamal Alameh and Dr. Magdalena Wajrak for their professional guidance during the course of my PhD studies. I would also like to thank those who provided technical and administrative assistance, enabling the completion of this project, particular Dr. Nur E Alam and Mr. Paul Roach. Additionally I would like to thank Edith Cowan University and the Electron Science Research Institute for the provision of scholarship funding, without which this project could not have been completed.

List of Abbreviations

IUPAC	International Union of Pure and Applied Chemistry
WE	Working Electrode
RE	Reference Electrode
FET	Field Effect Transistor
ISFET	Ion Sensitive Field Effect Transistor
M	Moles per litre
PDMS	Polydimethylsiloxane
PDADMAC	poly-diallyldimethylammonium chloride
PAMPSA	poly-2-acrylamino-2-methyl-1-propanesulfonic acid
RFMS	Radio Frequency Magnetron Sputtering
RTA	Rapid Thermal Annealing
PID	Proportional Integral Derivative
ISE	Ion Selective Electrode
OMC	Ordered Mesoporous Carbon
SEM	Scanning Electron Microscopy
PET	Polyethylene Terephthalate

List of Publications

1. W. Lonsdale, D.K. Maurya, M. Wajrak, K. Alameh, Effect of ordered mesoporous carbon contact layer on the sensing performance of sputtered RuO_2 thin film pH sensor, Talanta. 164 (2017) 52–56. doi:10.1016/j.talanta.2016.11.020.

2. W. Lonsdale, M. Wajrak, K. Alameh, Effect of conditioning protocol, redox species and material thickness on the pH sensitivity and hysteresis of sputtered RuO_2 electrodes, Sensors Actuators B Chem. 252 (2017) 251–256. doi:10.1016/j.snb.2017.05.171

3. W. Lonsdale, M. Wajrak, K. Alameh, RuO_2 pH Sensor with Super-Glue-Inspired Reference Electrode, Sensors. 17 (2017) 2036. doi:10.3390/s17092036.

4. W. Lonsdale, M. Wajrak, K. Alameh, Manufacture and Application of Solid-State RuO_2 Metal-Oxide pH sensor to Beverages, Talanta. 180 (2018) 277-281. doi:10.1016/j.talanta.2017.12.070

Abstract

The measurement of pH is undertaken frequently in numerous settings for many applications. The common glass pH probe is almost ideal for measuring pH, and as such, it is used almost ubiquitously. However, glass is not ideal for all applications due to its relatively large size, fragility, need for re-calibration and wet-storage. Therefore, much research has been undertaken on the use of metal oxides as an alternative for the measurement of pH.

Here, a solid-state potentiometric pH sensor is developed using ruthenium metal oxide (RuO_2). Initially, pH sensitive RuO_2 electrodes were prepared by deposition with radio frequency magnetron sputtering (RFMS) in a reactive oxygen plasma, onto screen-printed carbon based electrical contacts (substrates). These electrodes performed well, between pH 4 and 10, exhibiting Nernstian pH sensitivity, low hysteresis and low drift rate. However, these electrode were found to exhibit less than ideal properties outside this range (pH 2-12), though this could be overcome using a pH 12 conditioning protocol. Later, improved RuO_2 pH sensitive electrodes were developed and characterised. Elimination of the carbon substrate material resulted in electrodes that displayed excellent performance from pH 2 to 12, even without pH 12 conditioning.

Whilst this RuO_2 electrode displayed excellent pH sensing performance, RuO_2 along with all other metal oxide based pH sensors suffer from interference caused by strong oxidising and reducing agents. To reduce this interference, Ta_2O_5 and Nafion protective layers were studied. Using a combination of sputter deposited Ta_2O_5 (80 nm) and thermally cured drop-cast Nafion, an electrode was manufactured, which was immune to interference from dissolved oxygen, and resistant to stronger redox species. This electrode was found to outperform an unprotected RuO_2 electrode and was suitable for application in several common beverage samples.

In order to construct a potentiometric pH sensor a reference electrode is also required. Here, a pH in-sensitive reference electrode was developed by modification of the pH sensitive RuO_2 electrode with a porous polymer junction containing SiO_2. The reference electrode showed very low sensitivity to pH and KCl. The reference electrode provided a suitably stable potential over short periods of time, allowing accurate pH measurements to be made. The potential of the reference electrode was found to drift over longer time periods, however, this could be accounted for by recalibration.

The developed working and reference electrodes were then used to construct a pH sensor. The sensor displayed excellent performance between pH 2 and 6; close to Nernstian sensitivity (-55.3 mV/pH), linear response (R^2=1.0000) and excellent reproducibility (hysteresis <1 mV). The sensor was applied to several beverage samples, where it was shown to perform accurately, results within ±0.08 pH of a commercial glass pH sensor. The sensor develop here would be suitable for development into hand-held and in-situ type pH sensor devices.

Table of Contents

Chapter 1 – Introduction, Literature Review, Methods and Aims

1.1 Introduction

Sørensen [1] first introduced the concept of pH back in 1909. Today, along with mass and temperature, pH is one of the most frequently measured parameters [2]. For example, pH governs many biochemical reactions including the function of enzymes, therefore blood pH must be between 7.35 and 7.45 in order to maintain proper biological function [3]; heavy industries, such as extractive metallurgy, where refining processes are influenced by pH [4]; environmental applications, where the pH of natural-waters needs to be known in order to calculate alkalinity, an important parameter for the determination of water quality [5]; agriculture, where soil pH influences the growth rate of plants [6]; and in food production, where the control of pH is used to ensure the consistent manufacture of foods and beverages [7]. The measurement of pH even occurs domestically, where it is used to control the water quality of household pools and aquariums.

Due to the widespread measurement of pH, it is necessary to have a reliable means of measuring it, in a wide range of applications. The common glass pH probe is almost ideal for measuring pH and is used almost ubiquitously. Development of the glass pH sensor has led to the creation of specialised sensors for individual applications, ranging from high precision sensors for specialised environments, to cheaper hand-held devices for personal use, which are readily available from numerous manufacturers. However, glass is not ideal for all pH sensing applications, due to its relatively large size, fragility and the associated manufacture costs of working with such a material [8,9]. Therefore, much research has been undertaken on the use of metal oxides as a small-footprint alternative for the measurement of pH [8,9].

1.2 Theory and Literature Review

1.2.1 pH and Potentiometry

The International Union of Pure and Applied Chemistry (IUPAC) defines pH as the base-10 logarithm of the inverse, of the hydrogen ion activity in a solution, i.e.:

$$pH = -log_{10}[\alpha_{H^+}] \quad (1)$$

The definition of pH with respect to its activity in solution (as opposed to concentration) is advantageous, since potentiometry allows for the direct measurement of ionic activity [10].

Potentiometry involves measuring the electrical potential between two electrodes, known as the working (W.E.) and reference (R.E.) electrodes. Figure 1 shows a schematic representation of a typical potentiometric cell, consisting of two electrodes placed in solution, connected via wires to a

high impedance voltmeter [11,12]. According to the phase boundary potential model, where two materials meet, a phase boundary occurs and there is an associated shift in potential, also shown in Figure 1 [12,13].

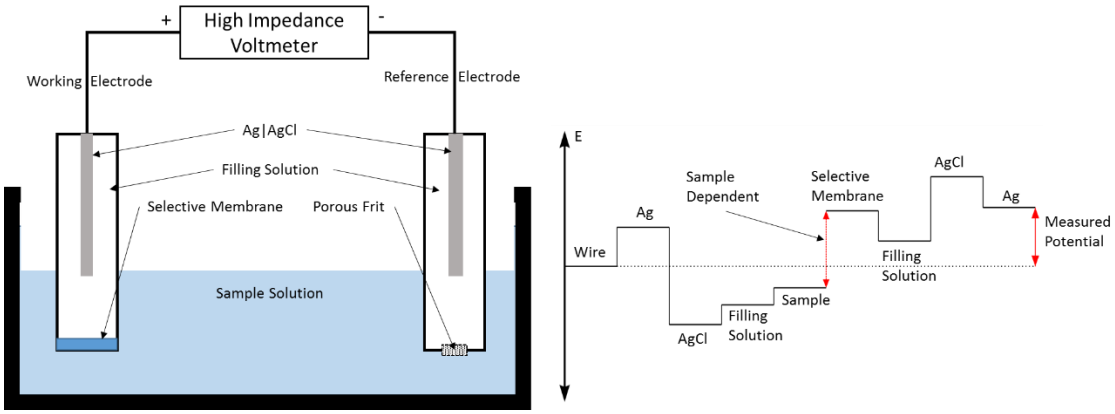

Figure 1 - Schematic diagram of a typical potentiometric cell, consisting of working and reference electrodes and a high impedance voltmeter. Along with a representation of the shift in potential that occurs at each phase boundary. Note that only the phase boundary of the working electrode is sample-ion depended, whilst the rest are constant.

If all phase boundary potentials in a potentiometric cell remain constant, except one, which is dependent on the concentration of an analyte ion in solution; using the Nernst equation it is possible to relate the potential difference between the working and reference electrodes to ionic activity:

$$E = E^0 - \frac{RT}{zF} ln \frac{\alpha_{(Solution)}}{\alpha_{(Electrode)}} \quad (2)$$

where E^0 is the standard redox potential (V), R is the universal gas constant (8.3144 $JK^{-1}mol^{-1}$), T is temperature (K), z is the charge of the species, F is the Faraday constant (96485 $Cmol^{-1}$) and $\alpha_{(Solution)}$ and $\alpha_{(Electrode)}$ are the activities of the analyte ion on the solution-side and electrode-side of the solution-electrode phase-boundary, respectively [12]. If $\alpha_{(Electrode)}$ remains constant and at a fixed temperature of 22 ^{O}C, then:

$$E = E^0 - 0.0583 \log[\alpha_{(Solution)}] \quad (3)$$

This results in a shift of 58.3 mV per 10 fold change in ion activity and is known as a "Nernstian" response. Potentiometric ion sensors exist for many ions, the following sections review and discuss the various kinds of pH sensitive working electrodes, along with several reference electrodes.

1.2.2 Glass pH Electrodes

The well-known glass pH sensor typically houses the working and reference electrodes in a single tube, making it convenient to use. This section briefly discusses the working electrode, whilst the reference electrode is discussed latter.

Glass pH electrodes consist of a thin membrane made from specially formulated H^+ ion selective glass, an internal electrolyte solution (3 M KCl) and an Ag|AgCl electrode (Figure 2). The difference in potential that occurs across the glass membrane reflects the difference in H^+ activity on either side of the membrane. Given the pH of the internal electrolyte remains constant, the pH of the solution can be determined, as per the Nernst equation (Equations 2 and 3). The glass pH electrode gives a linear response from pH 0 to 14 and is immune to virtually all interferences, apart from alkaline ions (Na^+ and to a lesser extent Li^+) at high concentration and pH (alkaline error), and very low pH (<1) (acid error), which are fairly uncommon in typical applications [14]. This makes glass pH electrodes almost ideal as pH sensors, and are therefore used almost ubiquitously. However, glass pH electrodes have several shortcomings.

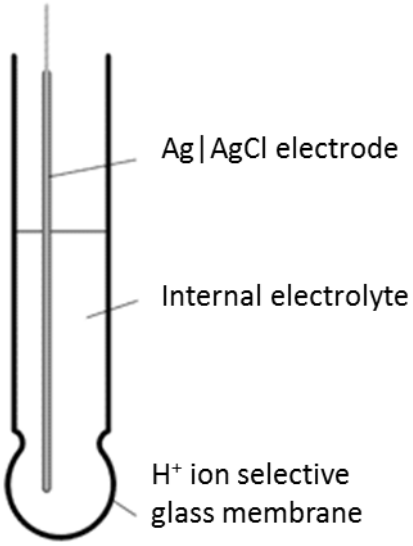

Figure 2- Schematic of a typical glass pH sensitive electrode, showing H^+ ion selective glass, an internal electrolyte solution and an Ag|AgCl electrode.

Glass corrodes at high pH, typically a zero potential (with respect to an Ag|AgCl reference) is achieved at 6.84 pH, but this increases slowly over time as the glass membrane corrodes. The surface of the glass membrane is hydrated with –OH groups and exists as a gel-like phase, due to dissociation of these surface sites the pH response can be slightly less than Nernstian. Glass pH probes typically do not operate above 130 ^{O}C [8]. Glass is fragile making it unsuitable for certain applications, such as in *in-vivo* studies (due to the risk of breakage) and is a limiting factor for sensor miniaturisation. Fragility of glass also contributes to the cost of manufacture. Internal liquid electrolytes also need to

be replaced, resulting in device maintenance. Therefore much work has been undertaken in the development of an alternative approach using an all-solid-state construction [8].

1.2.3 Solid State pH Electrodes

Many materials are known to respond to pH and can be grouped into several categories. Potentiometric pH sensors have been manufactured using conductive metal oxides; including metal-metal-oxide and metal-oxide-metal-oxide systems. An alternate technique exists using insulating metal oxides, which exploits the field effect transistor effect (FET) (not potentiometric). There are also potentiometric pH sensors constructed from metal-nitrides, conducting polymers, carbon materials, and liquid-hydrophobic membranes. This work focuses on the use of ruthenium oxide for the construction of a pH sensor, as such, an overview of each material is described, with more detail given to ruthenium and the closely related iridium oxide.

1.2.3.1 Metal-Metal Oxide

Metals that form insoluble hydroxides can be used for pH measurement. The most well-known example of this is the antimony electrode, which is typically used when the glass pH electrode is not suitable, such as in HF [15,16]. The potential of a metal-metal-oxide electrode depends on its half-cell reaction and the Nernst equation [8,17], for example:

$$Sb_2O_3 + 6H^+ + 6e^- \leftrightarrow 2Sb + 3H_2O \tag{4}$$

$$E = E^0 + \frac{0.059}{6}\log\frac{1}{[H^+]^6} = 0.152 - 0.0583pH \tag{5}$$

However, Sb-Sb_2O_3 electrodes are not stable over long periods of time, due to the formation of intermediate valance oxide states from reaction with dissolved oxygen [18]. The antimony oxide electrode typically does not reach the expected Nernstian sensitivity; this is reported as far back as 1924 [19] using a poured-melt Sb electrode, and recently, using nano-wires of antimony [17]. However, research has been undertaken to improve the electrode's stability, for example, by modification of antimony with the cation-conducting polymer Nafion [20].

Other metal-metal oxide systems reported include Sn, W, Fe, Ag, Cu and Zn [8]. Along with bismuth oxide, which has been reported for use in alkaline conditions [8]. Typically these electrodes do not achieve the expected Nernstian response, are limited to a narrow pH window and their potential is effect by anions present in solution [8]. However, recent work using tungsten has shown that, WO_3 sputter deposited at oblique angles achieves a close to Nernstian response of -57.7mV/pH. [21]. Tin oxide is also well reported in the literature, and has been used as a pH sensitive transducer in the construction of biosensors [22,23].

Metal-metal-oxide pH electrodes are advantageous in that they are made from relatively-cheap non-precious metals. However, these electrodes are not simple hydrogen electrodes and their potential is

determined by several simultaneous electrochemical processes [8] (such as corrosion and the cathodic reduction of oxygen [16]). A more suitable alternative to metal-metal-oxide pH sensors are those based on a redox couple between two oxidisation sates of the same metal, i.e. metal-oxide-metal-oxide pH sensors.

1.2.3.2 Metal Oxide – Metal Oxide (Iridium Oxide)

Pt group metal oxides have been shown to function as reversible hydrogen electrodes and can be used as pH sensors [8]. Oxides of Pt, Pd, Rh, Os, Ru and Ir have all been investigated [18,24]. Early works by Fog and Buck [18] and Kreider *et al.* [24] on conductive oxides identified Ir and Ru oxides as the most promising for pH measurement. However, IrO_2 was found to exhibit less sensitivity to redox agents, and higher stability, and as a result iridium has been extensively studied for many years [18].

Many techniques have been used to prepare iridium oxide pH sensitive electrodes, including thermal oxidisation [15], electro-oxidisation [25] and hot-melt oxidisation [26] of Ir wires; along with thermal decomposition of Ir^{3+} salts [27,28], electro-deposition [29,30] and reactive direct current sputtering (DCS) [31] and radio frequency magnetron (RFMS) sputtering [32], of IrO_2 on various substrates. Interestingly, thermal oxidisation of Ir metal results in a metal-metal-oxide system between Ir metal and $Ir(OH)_3$, whilst the other techniques, including thermal oxidisation of Ir^{3+} salts, form a metal-oxide-metal-oxide system [15]. In addition to this, the pH sensitivity of IrO_2 electrodes differs depending on the deposition technique used. IrO_2 can be split into two categories; anhydrous, which is produced mainly by sputtering [31,32] and hot-melt techniques [26], and hydrous, which is produced by electro-oxidisation [25] and electro-deposition techniques [29,30].

Anhydrous IrO_2 exhibits the typical Nernstian pH sensitivity expected for a metal-oxide-metal-oxide pH sensor [15]. The equilibrium reaction for electrodes made of anhydrous IrO_2 is:

$$IrO_{\frac{(x+n)}{2}} + nH^+ + ne^- \leftrightarrow IrO_{\frac{x}{n}} + \frac{n}{2}H_2O \tag{6}$$

which for simplicity can be written as:

$$2IrO_2 + 2H^+ + 2e^- \leftrightarrow Ir_2O_3 + H_2O \tag{7}$$

However, IrO_2 is known to partially hydrate over time and the reaction changes to:

$$IrO_{\frac{(x+n)}{2}}(H_2O)_{y+m} + nH^+ + ne^- \leftrightarrow IrO_{\frac{x}{2}}(H_2O)_y + \left(m + \frac{n}{2}\right)H_2O \tag{8}$$

which can be written as:

$$IrO_2 + 2H^+ + 2e^- \leftrightarrow IrO(H_2O) \tag{9}$$

Regardless, since the number of protons and electrons involved in each reaction are the same, the Nernst equation reads:

$$E = E^0 + \frac{RT}{2F} ln\left(\frac{\alpha[Ir^{III}]}{\alpha[Ir^{IV}].\alpha[H^+]^2}\right) \quad (10)$$

$$E = E^0 - \frac{2RT}{2F} ln(\alpha[H^+]) = E^0 - 0.0583pH \quad (11)$$

which gives the expected Nernstian response. The partial hydration of anhydrous IrO_2 is a slow process, in some cases it has been reported to take up to months [31]. It is therefore necessary to condition or pre-age electrodes before use. T. Katsube *et al.* [31] have reported a procedure whereby they boiled IrO_2 electrodes before use in deionised water for 30 minutes, whilst, others simply allowed electrodes to soak in pH 7 buffer for several weeks [15].

The pH sensitivity of hydrous IrO_2 electrodes is known to vary between 1 and 1.5 times Nernstian [15]. In order to explain this "super"-Nernstian pH response the effect of protonation and de-protonation without electron transfer has been used [29]. Electro-deposited hydrous IrO_2 forms a gel-like structure, existing as a "hydrated oxyhydroxide in a cross-linked open-polymetric chain" [15,29]. The many hydroxide sites can act as amphoteric sites, according to the site binding theory, which take-up or release protons without electron transfer [25]. Taking this into account, the equilibrium reaction for the potential of hydrous IrO_2 becomes [29]:

$$2IrO_2(OH)_{(2-x)}(H_2O)_{(2+x)}^{(2-x)-} + (3-2x)H^+ + 2e^- \leftrightarrow Ir_2O_3(OH)_3(H_2O)_3^{3-} + 3H_2O \quad (12)$$

For which the Nernst equation is:

$$E = E^0 + \frac{RT}{2F} ln\left(\frac{\alpha[Ir^{III}]}{\alpha[Ir^{IV}].\alpha[H^+]^{(3-2x)}}\right) \quad (13)$$

$$E = E^0 - \frac{(3-2x)RT}{2F} ln(\alpha[H^+]) = E^0 - 0.0583(1.5-x)pH \quad (14)$$

where "x" is a value between 0 and 0.5 [15]. This "x" value represents the degree of dissociation of the hydroxyl groups and was found to vary depending on the oxidisation state of the IrO_2 electrode [29]. Fully-reduced electrodes exhibit a pH sensitivity close to 58 mV/pH (x=0.5), whilst, fully oxidised IrO_2 exhibits a sensitivity close to 88 mV/pH (x=0). This accounts for the variety of sensitivity values reported in literature. Sensitivity values of 65 to 75 mV/pH are not uncommon for hydrous IrO_2 pH sensors, which can simply be attributed to a mixture of Ir^{III} and Ir^{IV} in the electrode. It has also been shown that reduced or partially reduced electrodes are not stable in ambient oxygen saturated solutions, due to the slow oxidisation of Ir^{III} to Ir^{IV}. However, when fully oxidised, the pH sensitivity of a hydrous IrO_2 electrode is stable [29].

The main drawback of Ir (and all other metal-oxide pH sensors [15]) is their sensitivity to redox species. Researchers have shown that both ferri- and ferro- cyanide completely supress the pH response of IrO_2 [18,33]. It has also been shown that when the interfering redox species is removed,

the pH response returns, however, the E^0 value is significantly lower [34]. This behaviour is attributed to a change in the composition of the iridium oxide film [34]. This limits iridium-oxide pH sensors to applications free from species that oxidise or reduce the electrode material, unless further modification of the sensor is undertaken.

Research by Kinlen *et al*. [33] has shown that a thin layer of thermally cured Nafion was able to protect an IrO_2 electrode from ferri-/ferrocyanide interference. However, the Nafion layer did not provide protection against all redox-active compounds; their sensor was still susceptible to interference from iodide and permanganate ions. The addition of Nafion to their IrO_2 electrode also increased the reaction time of their sensor in the neutral pH region. This was attributed to the presence of sulfonic acid sites that are not easily accessible, resulting in a lower degree of hydration, due to their increased hydrophobicity. These sites have a lower acidity (pK_a values of 6-9) resulting in a slower proton transfer rate through the material.

More recently, work by Li-Min Kuo *et al.* [32] has shown that modification of an IrO_2 electrode with a thin layer of sputtered Ta_2O_5 was able to eliminate potential fluctuations caused by dissolved oxygen. According to their work, the electrically insulating layer of Ta_2O_5 blocks the transport of electrons generated by oxygen in solution to the IrO_2 electrode. However, due to proton-electron double injection (the conduction of both electrons and protons across the interface) the current continuity across the interface is preserved, allowing the Ir^{III}/Ir^{IV} ratio to remain constant, resulting in a stable electrode potential. Which was observed as a low drift rate of <0.1 mV/h in both N_2 and O_2 saturated solutions.

Carroll *et al.* [34] developed a procedure for recovering from redox-interference. In their work, they used micro-fabrication techniques (sputtering and photolithography) to manufacture an array of 11 electrodes in a 1 cm^2 chip. Electrodes were made of Au and modified with IrO_2 using electro-deposition. The sensitivity and E^0 values of individual electrodes in the array were found to differ by 5.7 mV/pH and 100 mV, respectively. By applying a potential of +200 mV to the electrode with respect to an Ag|AgCl|KCl reference electrode using a potentiostat, it was possible to reduce the range of sensitivities to 2.3 mV/pH and the spread of E^0 values to 20 mV. This was used as a "self-calibration" procedure for the sensor array. By performing the +200 mV treatment it was possible to "re-set" the Ir^{III}/Ir^{IV} ratio of their electrodes to a value consistent to when it was calibrated. This procedure was also shown to restore the electrode to a consistent E^0 value after exposure to ferri-/ferro-cyanide. However, the procedure needs to be performed in the same pH buffer each time (pH 7).

Another notable example of a pH sensor constructed using IrO_2 has been reported by Sheng Yao *et al.* [26], who described a procedure for the hot-melt oxidisation of Ir wire using lithium carbonate. Notably, their electrode did not require conditioning, was long term stable (up to 2.5 years [35]) and

exhibited a Nernstian response. The excellent performance of this electrode was attributed to the presence of Li in the film. Wen-Ding Huang *et al.* [27] have reported a pH sensor based on IrO_2 manufactured using a Sol-Gel process. Their sensor employed an Ag|AgCl quasi reference electrode and a flexible polyimide substrate. Although this sensor exhibited sub-Nernstian sensitivity (51 mV/pH), the sensor was successfully developed into an array that displayed improved performance [28], and eventually developed into an implantable device for wireless monitoring of gastro-oesophageal reflux [36]. Bo Zhou *et al.* [37] have developed a multi-parameter sensor chip (pH, conductivity and temperature) for water quality assessment, which employed an electrodeposited IrO_2 electrode. Naroa Uria *et al.* [38] have successfully employed an electrodeposited IrO_2 film to detect pH changes caused by bacteria (E. coli.).

1.2.3.3 Metal Oxide – Metal Oxide (Ruthenium Oxide)

Early work by Fog and Buck [18] showed that Ir is less effected by interference from redox agents compared to other Pt group metal oxides. As such, many researchers have chosen Ir over Ru and the other Pt group metals for the construction of pH sensors. However, compared to iridium, ruthenium has the advantage of being cost-effective (Table 1 – Approximate US dollar values of Ru, Ir, Ag and Pt, from 2007-2017. Data from infomine.com.), although this is subject to market changes.

Table 1 – Approximate US dollar values of Ru, Ir, Ag and Pt, from 2007-2017. Data from infomine.com.

Metal	Price (USD/g)			
	Dec 2017	Min	Mean	Max
Ru	6	2	2.5	27
Ir	31	5	15	35
Ag	0.55	0.30	0.50	1.4
Pt	30	25	30	70

Fog and Buck [18] proposed five possible mechanisms for the pH sensitivity of electrically conducting metal oxides, namely, (i) ion exchange of surface –OH sites, (ii) redox equilibrium between two valencies, (iii) redox equilibrium involving only one phase, (iv) single phase oxygen intercalation and (v) steady state corrosion. Based on the observations that (i) redox agents caused shifts in potential (meaning that the composition of the material influenced potential); (ii) lack of interference from cations; and (iii) the known non-stoichiometric oxygen content of these metal oxides, the oxygen intercalation explanation (which assumed proton activity in the liquid phase and oxygen activity in the solid phase) was used to describe the pH sensitivity of RuO_2 electrodes. However, Pt group metal oxides were found to exchange protons with solution [39,40], while

investigation of the point-of-zero-charge and the exchange of tritium ions with RuO_2 revealed the following mechanism:

$$RuO_x(OH)_y + ze^- + zH^+ \leftrightarrow RuO_{x-z}(OH)_{y+z} \quad (15)$$

simplified to:

$$Ru^{IV}O_2 + e^- + H^+ \leftrightarrow Ru^{III}O(OH) \quad (16)$$

where the Nernst equation is:

$$E = E^0 + \frac{RT}{nF} ln\left(\frac{\alpha[Ru^{III}]}{\alpha[Ru^{IV}].\alpha[H^+]}\right) \quad (17)$$

$$E = E^0 + \frac{RT}{nF} ln\left(\frac{\alpha[Ru^{III}]}{\alpha[Ru^{IV}]}\right) + \frac{RT}{nF} ln\left(\frac{1}{\alpha[H^+]}\right) \quad (18)$$

Assuming nearby equal activates of Ru^{III} and Ru^{IV} (which approach 1 in the solid-state), the second term becomes zero and the potential of a RuO_2 electrode becomes:

$$E = E^0 - 58.3pH \quad (19)$$

where E is in mV at 22 ^{O}C. The thermodynamically calculated value for E^0 is 940 mV, however, in aqueous solutions a potential of 750 mV is measured [39,40].

RuO_2 is known to hydrate by the dissociative adsorption of water. This has been observed using X-ray photoelectron spectroscopy [41,42] and results in a "carpet" of –OH sites covering the RuO_2 surface. Experiments on the charge capacity of RuO_2 particles shows that hydroxide sites penetrate to a depth of 30 nm, but can remain in chemical equilibrium with solution [39]. Proton transfer without electron transfer at amphoteric –OH sites was used by J. Mihell *et al.* [43] to explain the sub-Nernstian sensitivity reported for their RuO_2 electrode, using similar logic to the super-Nernstian response observed for hydrous IrO_2. Whilst Kurzweil [8] has taken the effects of dissolved gasses into consideration to explain oxygen sensitivity. According to Kurzweil, in acidic solution, protons are released by the dissociative adsorption of water and super-acid OH groups, formally the oxidisation of hydrogen:

$$[Ru^{III}]_2O + H_2O \leftrightarrow 2[Ru^{IV}]O + 2H^+ + 2e^- \quad (20)$$

$$Formally: [Ru]H_2 \leftrightarrow [Ru] + 2H^+ + 2e^- \quad (21)$$

whereas, in basic solution, hydroxide sites are formed and bound in ruthenium cluster ions; formally the reduction of oxygen:

$$4[Ru^{IV}]O + 2H_2O + 4e^- \leftrightarrow 2[Ru^{III}]_2O + 4OH^- \quad (22)$$

$$Formally: [Ru]O_2 + 4e^- + 2H_2O \leftrightarrow [Ru] + 4OH^- \quad (23)$$

The predominance of dissolved oxygen and hydrogen in water, within the electrochemical stability window of water, can be estimated using the following equation:

$$H_2 + 2H_2O \leftrightarrow O_2 + 6H^+ + 6e^- \quad (24)$$

which gives a Nernst response of:

$$E = 819 - 59.1pH + 9.8log\frac{p(O_2)}{p(H_2)} \quad (25)$$

where E is in mV at 25 ^{O}C. Typically, these gasses are assumed to be present at constant concentration, and thus, the effects of O_2 and H_2 are omitted by most authors from the Nernst equation when describing the pH sensitivity of RuO_2.

Drift, ageing and hysteresis effects have all been reported for RuO_2 pH sensitive electrodes. A decrease in sensitivity and E^0 value over time is an indication of the ageing of the pH sensor. In some works a small decrease in sensitivity (<5 mV/pH) has been reported [24,44,45], whilst in another report, where electrodes were stored in strongly acidic solutions (<pH 2), a significant decrease in pH sensitively (32 mV/pH) was recorded [43]. However, in the majority of reports for RuO_2 pH sensitive electrodes this effect is not mentioned.

What is commonly reported, is a large decrease in E^0 value over the first few days of use. Typically E^0 values stabilise within a few days [45], however, for a thick-film RuO_2 electrode manufactured by screen printing a period of 20 days was required [46]. B. Xu *et al.* [45] concluded that the slow surface hydration of RuO_2 results in a drift in E^0 value and sensitivity, for their sputter deposited RuO_2 electrode with carbon nanotube substrate. On the other hand, Zhuiykov *et al.* [47,48] have stated that for their screen printed thick-film RuO_2 electrode, diffusion of H^+ through the material and the trapping of H_2 at grain boundaries and pores in the material is responsible. B. Xu et al. [45] have also linked the hysteresis observed for RuO_2 electrodes to, slow diffusion of H^+ between the inner and outer surface of the electrode and changes in the hydration of the RuO_2 material, whereas Zhuiykov *et al.* [47,48] explained the hysteresis of their RuO_2 electrode as being due to slow diffusion of H^+ into the material. A similar explanation of the hysteresis phenomenon has also been used by Bousse [49], where the hysteresis of ion sensitive field effect transistor devices (ISFETs) is attributed to the fast pH response, from easily equilibrated surface sites, followed by a slower response attributed to slower equilibration of difficult to access subsurface sites.

Redox interference is also problematic for RuO_2 electrodes. According to Kurzweil [8] redox agents, such as ascorbic acid, Fe^{2+}, sulphite, H_2O_2 and I_2, damage the electrochemical reversibility of RuO_2 electrodes at anodic and cathodic potentials, which indicates the role of adsorbed gases (H_2 and O_2) in the measured potential of RuO_2 electrodes. The E^0 value of RuO_2 electrodes is also known to shift after exposure to redox agents, similar to IrO_2 electrodes. However, Fog and Buck [18] stated that

RuO_2 maintains an almost Nernstian pH response slope when exposed to redox agents, whereas the other Pt metal oxides, i.e. Ir, do not.

The discussion above details theory regarding the pH sensitivity of RuO_2, whilst, Table 2 (below) chronologically summarises the various approaches adopted for the development of RuO_2 pH electrodes, over the last three decades.

Table 2 – Chronological summary of relevant literature using RuO_2 as a pH sensitive electrode for potentiometric measurements.

Author	Year	Summary
Fog and Buck [18]	1984	RuO_2 material used as supplied, 61.8 mV/pH, range 2-12, hysteresis 9 mV. All metal oxides are sensitive to redox agents, but, RuO_2 maintains an almost Nernstian pH response in the presence of redox agents whist other metal oxides do not.
K. Pásztor *et al.* [44]	1993	RuO_2 was electrochemically grown on gold wires. As prepared electrode exhibited 63.9 mV/pH, which decreased after 10 days storage in deionised water to 59.3mV/pH. There was also a shift in the E^0 value of 100 mV.
H. M^{c}Hurray *et al.* [40]	1995	RuO_2 glass composite sintered onto Pyrex glass substrate. E^0 value decreased by 65 mV over first 24 h, was aged for 14 days. pH 2 -12, 58-60 mV/pH, 25-30 mV hysteresis, 90 s response times and insensitive to dissolved oxygen.
K. Kreider *et al.* [24]	1995	Sputtered RuO_2 on SiO_2 and Al_2O_3 substrates. When sputtered at 230 ^{O}C, 54-60 mV/pH, E^0 0.89-0.93 V, across 4 electrodes. Exposure to pH 2 for 24 h decreases slope to 50-52 mV/pH and E^0 0.76-0.79 V. Neutral solutions decreased slope by 2-4 mV/pH. When sputtered at room temp, sensitivity was 54-59 mV/pH and E^0 0.85-0.89 V. Exposure to pH 2-3 buffers for 20h did not decrease sensitivity but exposure to pH 10 reduced slope to 54-55 mV/pH.
J. Mihell *et al.* [43]	1998	Hydrated RuO_2 was screen printed in a polymer matrix onto alumina substrates. Sensitivity dropped to 32 mV/pH if stored in HCl for 60 days; whilst, those stored in KOH, pH 6 buffer and water remained constant. The decrease in sensitivity for the acid stored electrodes was attributed to

		the take-up or release of protons without electron transfer at amphoteric RuO(OH) sites. This is similar to the explanation of the super-Nernstian response observed for hydrous IrO_2.
S. Zhuiykov [47]	2008-2011	Sintered RuO_2 nano-particles which were screen printed onto platinised alumina substrate. Linear pH response from pH 2 – 13, 58 mV/pH at 23 ^{O}C, with 1-2 s response time at 23 ^{O}C. However, response time increased greatly at lower temperatures, 8-10 min at 9 ^{O}C. Their electrode was also sensitive to superoxide ions (O_2^-) and could measure dissolved oxygen from 0.6 to 8.0 ppm. This RuO_2 electrode was used in the development of a sensor array for the measurement of water quality parameters; pH, temperature, dissolved oxygen, conductivity and turbidity [46]. Repose of the RuO_2 electrode was found to drift substantially over the first month, and was linked to trapping of hydrogen at the grain boundaries or micro-pores in the screen-printed nano-structured material. Doping of RuO_2 thick films with Pt was also studied [48]. Doping RuO_2 with 20 mol% of ZnO was found to increase dissolved oxygen sensitivity and reduce pH sensitivity [50]. Whilst, doping RuO_2 with Cu_2O was found to improve response times [51].
Yi-Hung Liao *et al.* [52]	2008	Sputter deposited array of 4 RuO_2 electrodes on Si wafer. Sensitivity of 55.64 mV/pH with 0.38 mV/h drift rate and 2.2-4.36 mV hysteresis. Reported that exposure to 720 lumen of light at pH 7 shifts response by 16.8 mV. This sensor was further developed by modification of the RuO_2 with enzymes to create a bio-sensor for the detection of glucose and uric acid [53]. It is unclear if the authors of this paper used potentiometric or FET based detection, likely FET-based given the reported light sensitivity.
Chou and Hsia [54]	2009	Employed an array of 8 sputter deposited RuO_2 electrodes on Si substrate. They achieved sensitivity of 56 mV/pH from 1-13, with 1.6 mV/h drift-rate and 1.1 mV hysteresis. Attributed good results to the multiple electrode sensor array, which minimises variations between sensors.
M. Brischwein	2009	Sputter deposited RuO_2 on Ti/Pt electrical contacts on ceramic substrate. Sensor chip was designed for in-vitro cell studies due to RuO_2's

et al.[55]		biocompatibility. Their sensor was approximately linear between pH 5.5 and 11, 52 to 58 mV/pH, 1-2 mV/h drift rate, across 15 sensors.
Bin Xu *et al.* [45]	2010	Sputtered RuO_2 on vertically aligned carbon nanotubes, 55mV/pH from pH 2-12, E^0 value drifts 80 mV and slope by 2.3 mV/pH over 1 day, was stable by day 2. This ageing was linked to changes in surface hydration. Stated that there is little explanation of hysteresis other than slow diffusion of H^+ between inner and outer electrode surface area and slow changes in hydration. Hysteresis between 5.1 and 10.2 mV, 40 s reaction time at basic pH.
M. Kahram *et al.* [56]	2013	Hydrous RuO_2 deposited by a Sol-Gel method on multi-wall carbon nanotubes. Sensitivity of 63 mV/pH from 2-12 pH with response time less than 50 s.
Jung-Chuan Chou *et al.* [57]	2015	Sputter deposited RuO_2 onto flexible polyethylene terephthalate (PET) substrates with screen printed silver paste electrical connections. Sensitivity of 59.66 mV/pH, R^2=0.995 from pH 1-13. Was used to manufacture a glucose bio-sensor, by immobilisation of glucose oxidase on the RuO_2 surface using Nafion.
L. Manjakkal *et al.*	2013-2017	Has authored a series of papers developing screen printed thick film RuO_2 pH sensors. Results using "off-the-shelf" resistive RuO_2 pastes gave sensitivities of 57-61 mV/pH [58]. A thick-film conductometric pH sensor was also developed using RuO_2 paste [59]. Reduction of Ru content (to reduce device cost) was investigated; addition of TiO_2 [42], SnO_2 [41] and Ta_2O_5 [60] to the sensor material were all investigated. Sensors employing 30 % Ta_2O_5 exhibited a 58 mV/pH sensitivity, pH 2-11 and hysteresis between 3-10 mV [61,62].
Sardarinejad and D. Maurya *et al.*	2013-2015	Manufacture a pH sensor based on a thin film of RuO_2 deposited on screen-printed Pt using radio frequency magnetron sputtering (RFMS) and a quasi Ag|AgCl reference electrode [63]. After optimisation of material thickness (300 nm) [64] and deposition gas composition (80% Argon, 20% Oxygen) [65], they report a sensor with super-Nernstian response (72.5 mV/pH) [66], though their sensor exhibited significant

		drift (40 mV over 10 min) and hysteresis (up to 20 mV), at 22 ^{O}C. They also applied this sensor to the measurement of engine oil acidity [67].

Based on Table 2 and the discussion above, it is clear that a significant amount of work has been undertaken using RuO_2 as a pH sensitive material. However, several gaps in this literature can be identified. Firstly, there are inconsistencies reported with regard to aging effects, i.e. the change in sensitivity and E^0 value over time, which could be due to the variety of manufacture processes and substrates used. Additionally, a thorough study of the redox sensitivity properties of RuO_2 and combating redox interference for RuO_2 pH electrodes is lacking. Finally, due to this interference, there are few reports of RuO_2 pH sensitive electrodes being applied to real samples, other than relatively simple sample matrices, such as fresh surface waters.

1.2.3.4 Ion Sensitive Field Effect Transistors

Another group of metal oxide based pH sensing devices use insulating metal oxides. Here however, the potential drop caused by protonation/de-protonation of active surface sites (-OH) at the interface between an electrically insulating oxide and a solution is measured as a shift in the flat-band voltage of the electrolyte-insulator structure, which is entirely different to the potentiometric electrodes described thus far [49]. Devices that employ this effect are known as ion sensitive field effect transistors (ISFETs). ISFETs are mentioned here since there is some overlap in the literature regarding the theory used to describe the pH sensitivity of ISFETs and potentiometric metal-oxide-metal-oxide pH sensors [8,41].

The pH sensitivity of an ISFET is determined by the electrolyte insulator interface. Using the site-dissociation model and the Gouy-Chapmann-Stern theory, Bousse [49] describes the change in potential at an electrolyte-insulator interface in terms of pH:

$$\psi_0 = \left(\frac{2.303kT}{q}\right)\left(\frac{\beta}{\beta+1}\right)\left(pH_{pzc} - pH\right) \tag{26}$$

where ψ_0 is the potential drop at the electrolyte insulator interface, k is the Bholtzmann constant, T is temperature, q is charge, pH_{pzc} is the point-of-zero-charge (the pH at which the insulator is neutrally charged) and β is a sensitivity parameter, which is proportional to the density of active surface sites. This predicts a Nernstian response near the point-of-zero-charge, given a sufficient density of sites [49] and that the hysteresis and drift of ISFET devices are influenced by changes in active-site density [68], though, slow equilibration of "buried" sub-surface –OH sites are also responsible for hysteresis [69].

ISFETs are well reported in literature and have been manufactured using Al [68], Ta [70,71], Zr [71], Si [71], Zn [72], Hf [73] and Sn [22] oxides, as well as some nitrides e.g. Si_3N_4 [74]. However,

ISFETs require a reference electrode to set the potential of the electrolyte-insulator interface, so that shifts in the flat-band voltage can be measured [49]. This measurement set-up is more complex than potentiometry and therefore the use of an ISFET device did not fit the criteria for possible future applications of this project.

1.2.3.5 Nitrides, Conducting Polymers, Carbon and Liquid-Hydrophobic Membranes

Materials other than metal-oxides have also been investigated for the construction of solid state potentiometric pH sensors. These include metal nitrides, conducting polymers, nano-carbon materials and solid-contact liquid-hydrophobic membrane electrodes.

Electrically conducting polymers have been used to manufacture pH sensors, the most frequently used are polypyrrole [75] and polyaniline [76,77]. Often the expected Nernst response is not achieved and slightly non-linear pH response is obtained [76,77]. However recent works combining nano-fabrication techniques and polyaniline have shown that this can be overcome. J. Yoon *et al.* [78], electrodeposit polyaniline onto a gold-coated flexible nanopillar structure. Their sensor was Nernstian form 2-12 pH, 2mV hysteresis and exhibited an almost instantaneous reaction time due to the nanopillar structure.

Typically, metal nitrides are more frequently used to manufacture ISFET type pH sensors. However, they have been used to manufacture potentiometric pH sensors. A notable example of this has been reported by M. Liu *et al*. [79] who manufactured a pH sensitive TiN nanotube array. First Ti is anodically oxidised to TiO_2, then reduced to TiN at 900 ^{O}C in a nitrogen/hydrogen atmosphere. Though a sub-Nernstian (55.3 mV/pH, pH 2-11) response was reported, the electrode was consistent, with very low hysteresis and drift. Very slight interference from K^+, Na^+, Cl^- and F^- was reported with shifts of 3-8 mV reported for 1 mol/L additions.

Another approach for pH sensing based on using nano-carbon materials has been reported by Cheng *et al.* [80], where a single-walled carbon nanotube thin film was prepared using a vacuum filtration method, then patterned to create electrodes. The electrodes reached the expected Nernstian sensitivity (pH 3-11), however, the linearity was poor over this range (R^2=0.985).

Liquid-hydrophobic membranes are have also been reported as potentiometric working electrodes [81], where, the concentration of analyte ion inside the membrane is buffered, using an ionophore [12,82,83]. For pH sensitive liquid-hydrophobic membranes, the ionophore tridodecylamine is typically used, and due to its protonation constant, the pH working range is limited to pH 2-9 [84].

1.2.4 Reference Electrodes

In order to make potentiometric measurements a reference electrode is required. The reference electrode must provide a stable potential that is unaffected by ions in the test solution, so that the potential of the working electrode can be accurately related to analyte ion concentration [10]. This makes the reference electrode as important as the working electrode, if one wishes to manufacture a reliable potentiometric sensor. Reference electrodes are most commonly manufactured using silver-silver chloride (Ag|AgCl), however other approaches are possible.

1.2.4.1 Silver – Silver Chloride

The standard hydrogen reference electrode is obviously impractical for most measurements, due to the use of hydrogen gas. Therefore, the silver-silver chloride reference electrode is a commonly used alternative [10,85]. The most basic Ag|AgCl electrode is constructed by simply chlorinating silver metal, using NaOCl, $FeCl_3$ or electroplating in HCl solution. However, this results in a quasi-reference electrode and its potential is actually determined by the concentration of Cl^- ions in solution, i.e.:

$$AgCl + e^- \leftrightarrow Ag + Cl^- \tag{27}$$

$$E = E^0 - \left(\frac{RT}{nF}\right)\ln[\alpha_{Cl^-}] + \left(\frac{RT}{nF}\right)\ln\frac{\alpha[AgCl]}{\alpha[Ag]} \tag{28}$$

$$E = E^0 - 59.3[Cl^-] + 59.2(k) \tag{29}$$

where "k" represents the ratio of Ag to AgCl. However, this sensitivity to Cl^- is eliminated by maintaining a stable concentration of Cl^- ions at the surface of the AgCl electrode [86].

In commercial glass double junction reference electrodes, a stable concentration Cl^- is maintained using concentrated (3.0 M) KCl electrolyte solution, which is linked to the test solution via a porous frit. Typically, a second electrolyte and frit surrounds this to prevent contamination of the electrolyte solution with sample ions. KCl is used due to the nearly equal ionic mobility of K^+ and Cl^-, which minimises the formation of a junction potential, due to the slow but equal leaching of K^+ and Cl^- (Figure 3).

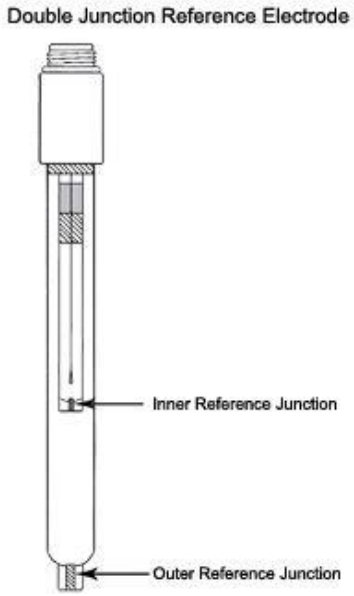

Figure 3 – A diagram of an Ag|AgCl|KCl double junction reference electrode showing the inner and outer junctions.

The glass double junction reference electrode is extensively used in electrochemistry. However, due to the use of glass and liquid electrolytes, the glass reference electrode is not suitable for certain applications or for miniaturisation. Therefore, significant research has been undertaken on this problem and there are many reports of solid-state reference electrodes in literature. In general, these electrodes consist of an electrical contact, a silver electrical track, a silver chloride working area, a KCl electrolyte layer, to prevent Cl^- sensitivity, and a junction/protective layer, to prevent loss of KCl, Ag and AgCl. Design choices for each component are summarised below in Table 3.

Table 3 – Summary of the design choices for typical Ag|AgCl solid state reference electrodes.

Component	Description
Electrical contact and track	Are usually made of silver due to its excellent conductivity and for simplicity, since the working area must also be silver.
Working Area	The silver working area can be sputtered, screen printed or electroplated [85]. No significant difference in performance between these methods is reported in literature. However care must be taken to ensure that there is sufficient silver present so that not all of it is converted to AgCl during the chlorination stage, which can occur for thin sputtered films (<100 nm) [85].
Chlorination	Achieved using chemical reaction with $FeCl_3$ [87] or NaOCl [88] and via

	constant current or constant voltage electroplating in chloride salt solution [89–91]. Alternatively, AgCl paste can be screen printed directly onto Ag [92].
Electrolyte Layer	Various KCl electrolyte layers have been applied to the AgCl surface to prevent Cl^- sensitivity. These include gels [93], polymers [94–97] and glasses [42,61,86,98] all loaded with KCl [86,92,93]. Of these, gels are prone to poor performance at high temperatures, whilst glasses require high temperatures during manufacture [86,92,93]. All electrolyte layers are prone to dissolution of KCl which results in potential drift and Cl^- sensitivity over time [86,92,93].
Protective Layers	Protective layers are applied to the electrolyte layer to prevent loss of KCl. These layers usually consist of a non-conducting glass or polymer [86]. Nafion has been used to contain Cl^-, since it is cation conductive, Cl^- will remain at the electrode's surface [33,85,99]. Whilst more recently graphene oxide has been used to prevent loss of AgCl, although its effects on Cl^- sensitivity was not tested [87].
Junctions	Junctions consist of a small opening in the protective layer. This allows electrical connection with the solution, whilst slowing the rate of KCl loss [100]. Some designs have used polydimethylsiloxane (PDMS) [100,101] or chloroprene [93] to create a barrier preventing loss of KCl, which greatly increases electrode stability.

A simpler approach for the construction of a solid-state reference electrode can be achieved if the KCl loaded electrolyte layer and protective layers are combined. A notable example of this is reported by T. Guinovart *et al.* [102]. In their work, a solution containing polyvinyl butyral, Ag, AgCl and KCl is drop cast on a carbon substrate. This electrode performed well over a 4 month period, with low drift (90 μV/h). The long term stability of this electrode was attributed to the formation of nano-pores at the surface of the PVB material. The nano-porous structure permitted the very slow leaching of KCl. This was developed further and applied for use in several sensors (Figure 4); including a bandage based pH sensor [103], an ammonium sensor and a sodium sensor for measurement of sweat [104,105].

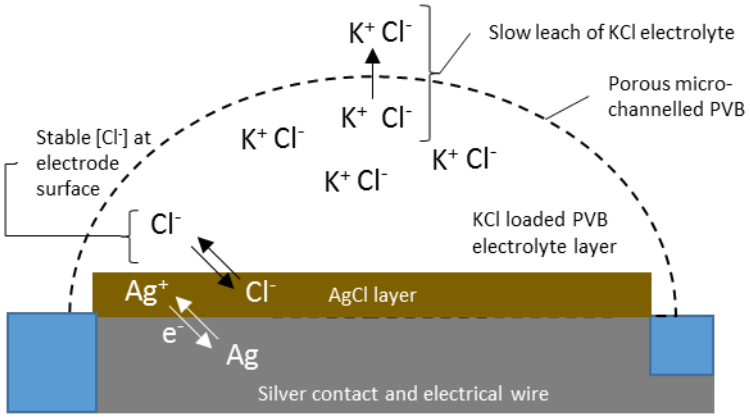

Figure 4 – Diagram of a solid-state Ag|AgCl reference electrode, reported by T. Guinovart *et al.*, showing the Ag layer, the AgCl layer and stable Cl^- concentration at the electrode surface due to nano-porous PVB loaded with KCl.

1.2.4.2 Other Reference Electrodes

There are also other approaches for the manufacture of solid-state reference electrodes. For example, pH sensitive IrO_2 electrodes have been used as a reference electrode in some biosensors [85]. If the pH of a test solution is buffered, the IrO_2 electrode's potential is stable and can therefore function as a pseudo-reference electrode [85]; which is not useful for the construction of a pH sensor.

For the construction of pH sensors, others have tried using "poor" pH sensitive materials, such as; carbon materials, bronzes [8] and conducting polymers [106–108]. These materials are engineered to exhibit a significantly less than Nernstian response to pH, allowing one to make differential measurements between a highly sensitive pH electrode and the "poorly" pH sensitive reference electrode [8]. However, these materials typically suffer from high hysteresis, instability and a small pH working range, which results in a poor quality pH sensor, prone to error form the reference electrode [8].

A different approach has been reported by J. Noh *et al.* [109], where the pH at the surface of a nano-porous Pt electrode is made constant using an alternating poly-electrolyte junction. The surface of the electrode is covered by poly-diallyldimethylammonium chloride (PDADMAC), which is then linked to the test solution via a narrow junction consisting of two alternating layers of poly-2-acrylamino-2-methyl-1-propanesulfonic acid (PAMPSA) and PDADMAC. Due to the alternating layers of cationic (PDADMAC) and anionic (PAMPSA) conducting polymers mass transport across the junction is suppressed but ionic conductivity is maintained. The electrode was reportedly very stable, with less than 1 mV of drift over 50 h and showed very low pH sensitivity with 2 mV difference between pH 2 and 12.

Liquid-hydrophobic membranes have also been used to construct reference electrodes. Here, compounds, incorporated into the hydrophobic membrane, leach slowly into sample solution and

become the potential determining ion for the electrode [110]. Compounds such as KCl and ionic liquids have been used, however, these suffer from fast leeching rates and pH sensitivity, respectively [111]. More commonly a moderately lipophilic compound is used, e.g. tetraalkylammonium tetrakis(4-chloro-phenyl)borate [110]. All solid-state designs for reference electrodes have been achieved using conducting polymer electrical contacts, however, high surface-area carbon contact material (meso-porous carbon) buffered with a Co^{II}/Co^{III} redox system produce electrodes with consistent E^0 values and low potential drift [13].

1.3 Project Aims and Rationale

The aim of this project is to manufacture an all-solid-sate pH sensor with the view of developing a sensor that is robust, simple to manufacture, easily miniaturised, relatively cheap to produce and is capable of measuring pH in a wide range of matrices. In order to achieve this aim, potentiometric measurement was chosen, because the measurement of voltage is relatively simple, which was deemed desirable for possible future applications.

Sputter deposited RuO_2 was selected for manufacture of an all solid state pH sensitive working electrode, due to the relatively lower cost of ruthenium compared to iridium and its demonstrated performance as a pH sensor. Additionally, a thorough study of the redox sensitivity properties and combating redox interference for RuO_2 pH electrodes is lacking in literature. Sputter deposition was selected since RFMS is able to manufacture films with high purity, known stoichiometry/composition and with well-controlled thickness; which is advantageous for investigation of the material's properties.

For manufacture of the reference electrode, it was desired that this process be as simple as possible, using similar techniques as the working electrode. The purpose of this was to keep the manufacture process of the pH sensor as simple as possible for potential future applications. However, beyond this, there were no specific specifications for the reference electrode to meet, other than it provides a suitably stable and interference-free potential for the potential of the working electrode to be measured against.

1.4 Research Outline

Based on literature review, the most recent work using RuO_2 to manufacture pH sensors, was conducted by A. Sardarinejad *et al*. and D. Maurya *et al*., who reported a pH sensor consisting of 300 nm RuO_2 film sputtered on a commercially available screen printed Pt substrate, with quasi Ag|AgCl reference electrode. This work was used as the basis for the development of an all solid state pH electrode.

In this thesis, the first step in the development of a suitable pH sensitive RuO_2 electrode was to investigate the effect of substrate on the performance of the RuO_2 electrode. Additionally, in order to reduce cost of the material components of the sensor, the screen printed Pt substrate was substituted for screen printed carbon. This investigation is reported in Chapter 2, where the use of two-different types of carbon was investigated, "regular" screen-printed carbon and screen-printed ordered-meso-porous carbon (OMC). Based on work in Chapter 2, OMC was selected as a substrate material for construction of RuO_2 pH sensitive working electrodes.

The next step undertaken was to investigate the RuO_2 layer on the performance of the electrode. This is explored in Chapter 3, where the thickness of RuO_2 sputter deposited on OMC substrates is optimised and the effects of redox agents (ascorbate and permanganate ions) and conditioning pH is investigated for the working electrode, demonstrating a good performance and outlining the limitations of the developed working electrode.

In order to manufacture a pH sensor, a reference electrode was needed. In Chapter 4, the RuO_2 pH sensitive working electrode is further modified and developed into a reference electrode. This reference electrode is remarkably simple in construction and could be suited to the manufacture of a low cost device. Using the developed working and reference electrodes a pH sensor is constructed and successfully applied to certain beverage samples. In addition, the limitations of the developed sensor to certain samples due to redox interference is discussed.

To better examine redox interference a new design was implemented for the RuO_2 electrode. In Chapter 5, a more durable RuO_2 electrode is manufactured consisting entirely of sputter deposited RuO_2 on a non-conducting Al_2O_3 substrate. This is advantageous for the investigation of the pH and redox sensing properties of RuO_2, enabling previously-unnoticed effects of the carbon substrate material to be eliminated. In addition the use of Ta_2O_5 and Nafion protective layers are investigated for the minimisation of redox interference.

In Chapter 6, the working electrode designed in Chapter 5 is further modified using an approach similar to that reported in Chapter 4 to manufacture a reference electrode. These working and reference electrodes are then used as a solid state pH sensor and successfully applied to several beverage samples.

1.5 Techniques and Metrics

Details of electrode manufacture and the procedures used to assess electrodes are given in individual chapters. This section gives a brief overview of the RFMS, laser cutter/engraver, annealing system, scanning electron microscopy and cyclic voltammetry systems used, along with a more detailed explanation of the metrics used to assess electrodes.

1.5.1 Electrode Manufacture

The technique used for metal-oxide deposition was RFMS, the system used was a Korea Vacuum Tech KVS-2004L (Figure 5). Deposition parameters are detailed in individual chapters. Briefly though, substrates were cleaned using an appropriate solvent (usually iso-propyl alcohol) in an ultra-sonic bath for 15-30 minutes, then completely dried on a hot plate at 120 ^{O}C. Sputter deposition areas were defined using a stencil (shadow mask). Then substrates were mounted in the RFMS and the deposition chamber brought to high-vacuum (<5×10^{-6} Torr) and deposition carried out using parameters specified in individual chapters.

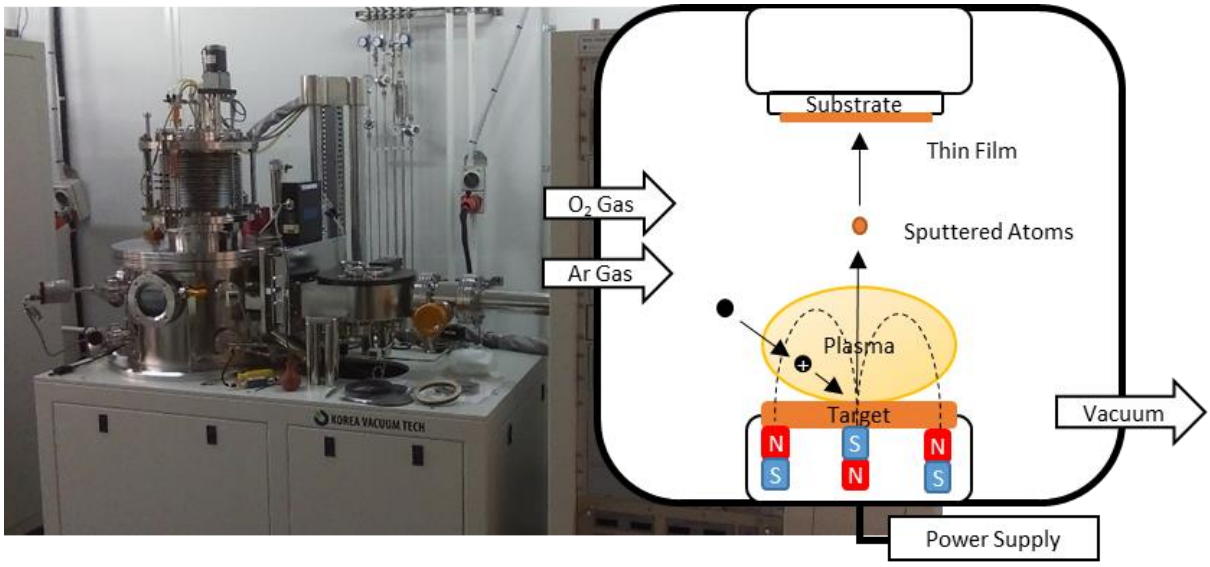

Figure 5 – RFMS system used for deposition of RuO_2 and Ta_2O_5. Inset showing a simplified schematic of the deposition process.

A Trotec Speedy 360 flex laser cutter engraver was used for etching RuO_2 on Al_2O_3 substrates, manufacturing acrylic-wells and manufacturing stencils for sputter deposition (Figure 6). Laser setting are detailed in appropriate chapters, or where not stated the manufactures recommended laser settings are used.

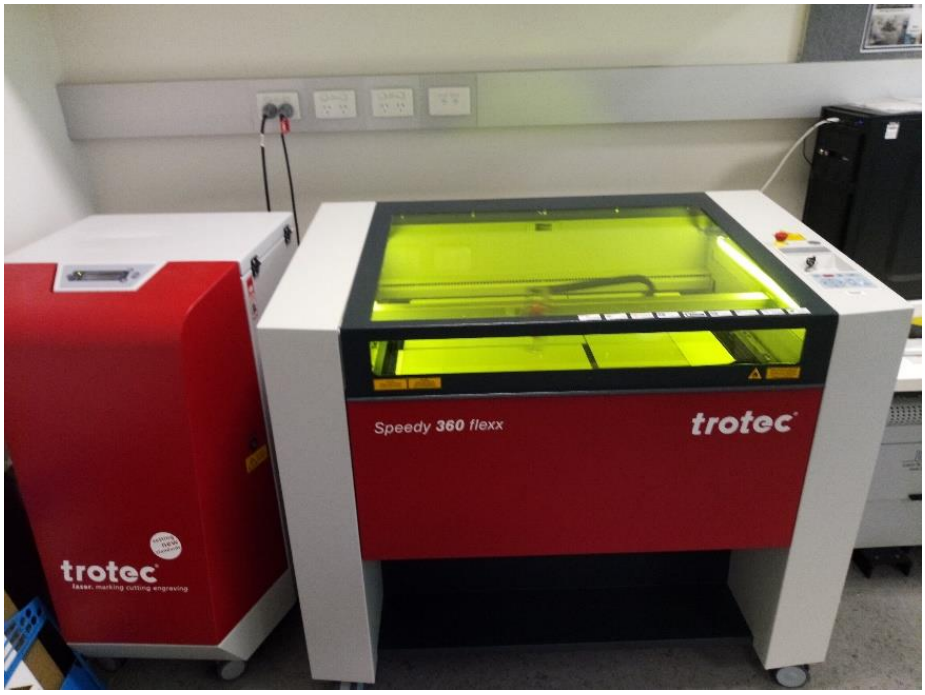

Figure 6 – Laser cutter/engraving system used for etching RuO_2, manufacturing acrylic-wells and stencils.

Rapid Thermal Annealing (RTA) was used to thermally cure Nafion. The system used was a Korea Vacuum Tech KVR-4000 (Figure 7). The system is controlled using a proportional–integral–derivative controller (PID). To cure Nafion the temperature set-point was set to 250 ^{O}C, with PID settings of P=6, I=0 and D=0. This resulted in a 30 s heating period with temperature stabilising at 230 ^{O}C. It should be noted that these PID settings are not typically how the devise is intended for use, however, this proved sufficient for the work conducted here.

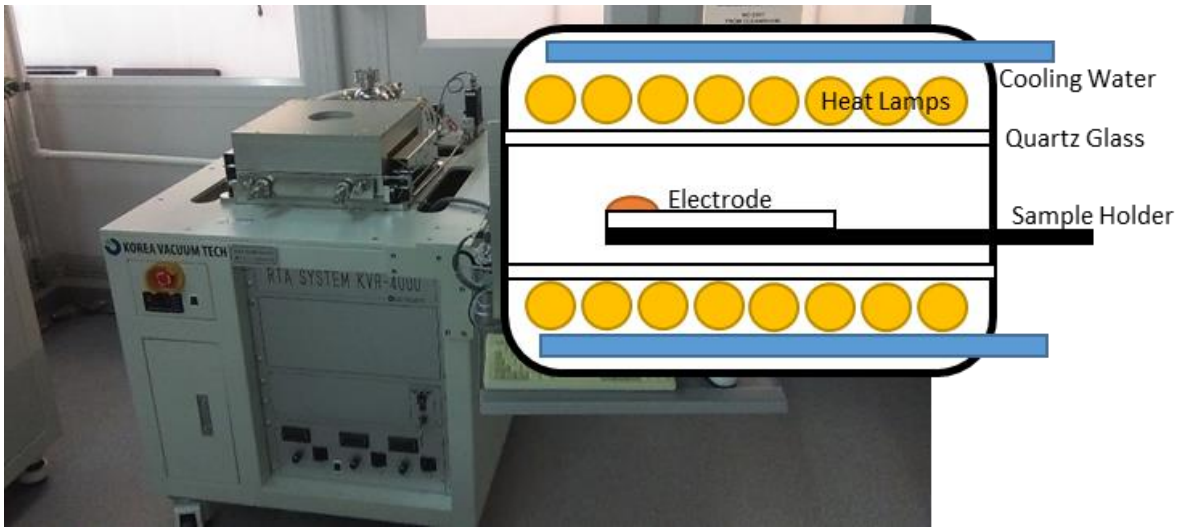

Figure 7 – RTA system used to thermally cure Nafion. Inset showing a schematic diagram of the annealing process

Scanning electron microscopy (SEM) was used to examine the morphology of developed electrodes. The instrument used was a Hitachi SU3500. Samples were cleaned using isopropyl alcohol and completely dried on a hotplate before being mounted with carbon tape to the specimen stub. Images were captured using secondary electron detection and settings (beam power and magnification) are displayed on individual images. Cyclic voltammetry was performed using a Modern Water PDV6000plus voltammetric instrument fitted with an Ag/AgCl reference electrode and Pt wire auxiliary electrode. Measurements were made in 0.5 M H_2SO_4 from 0 to 800 mV at sweep rates from 3.0 to 50 mV/s.

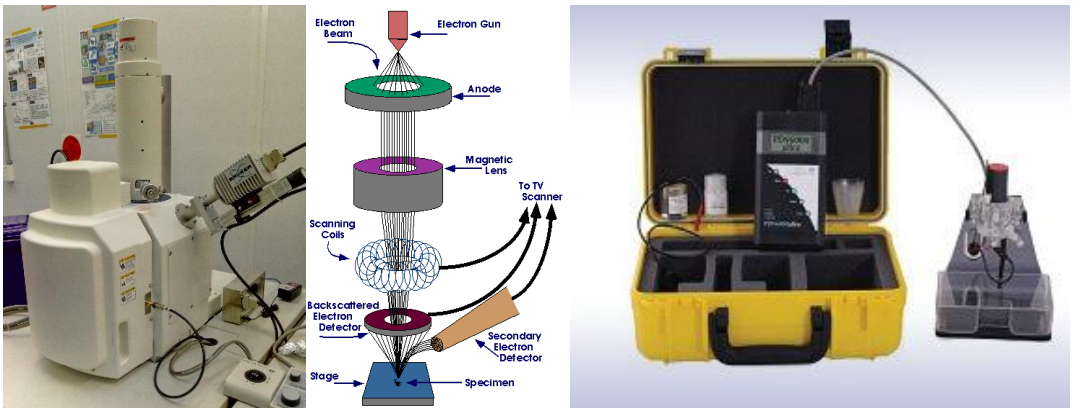

Figure 8 – SEM instrument used to examine morphology of electrodes (left), with a schematic representation of the SEM imaging process (middle) and voltammetric instrument used for cyclic voltammetry measurements (right).

1.5.2 Data Collection and Processing

The potential between working and reference electrodes was measured using an Agilent 34410A high performance digital multimeter using the high-impedance voltage setting (Figure 9). Data loops were generated by recording potential in pH buffer solutions for a specified amount of time (i.e. until the electrode has equilibrated), then changed by hand to the next test solution. Electrodes were not rinsed between test solutions, as this altered reaction times, and excess buffer solution was removed using a blast of air. A preliminary test using a commercial glass pH sensor found that there was no measurable carryover between measurements, due to the buffering capacity of the test solutions.

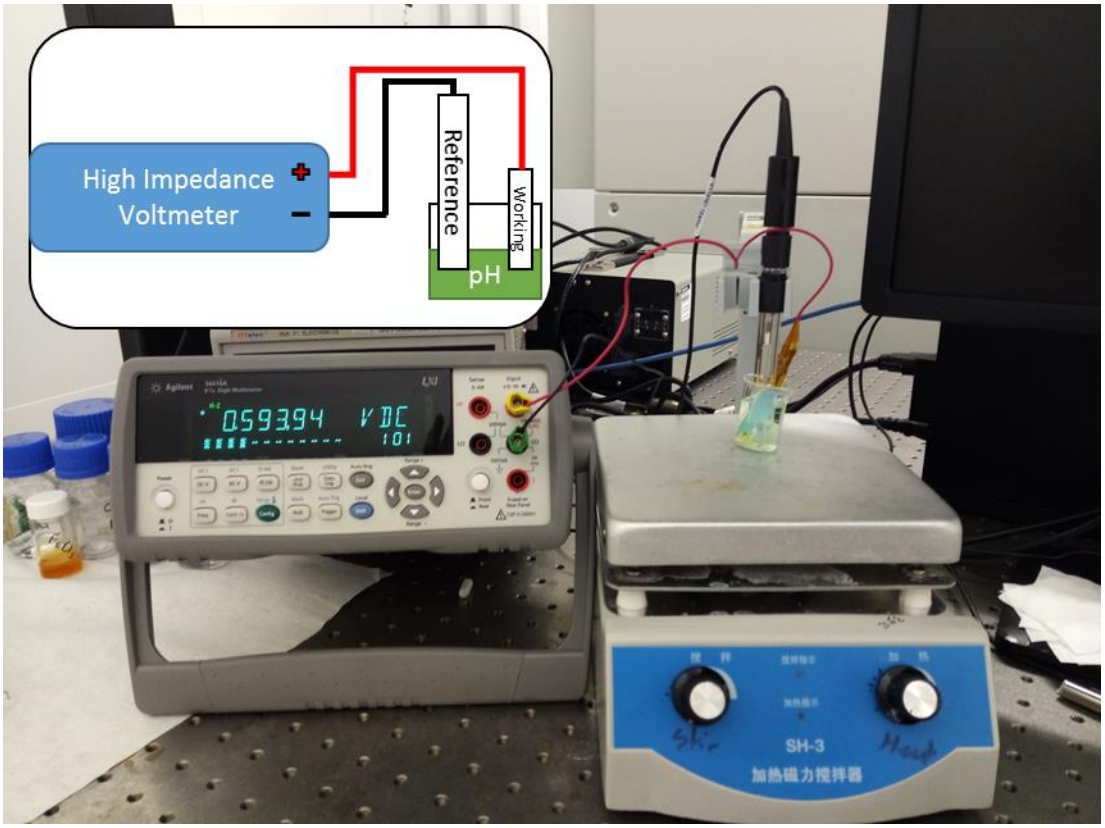

Figure 9 – Potentiometric measurement set-up. Shown is a glass double junction reference electrode and a RuO_2 working electrode in pH 7 buffer, connected to a high impedance voltmeter. Inset, showing a schematic representation of the setup.

The generated data loop was used to determine sensitivity, E^0, drift, hysteresis and reaction time for the electrodes. Data from the last 30 s of individual potential recordings is typically averaged, giving individual measurements for each pH solution. Respectively, the Sensitivity and E^0 values are the slope and intercept values of the linear pH vs. potential calibration plot, generated using these measurements. Hysteresis is the difference in potential between consecutive measurements at the same pH, after exposure to another pH solution. Drift is calculated using the line of best fit for the data over the test interval. Reaction time is defined as the time taken to reach within a specified value of the stable potential. Each of these metrics is further defined in individual chapters, and are also summarised graphically below with, an exaggerated example (Figure 10).

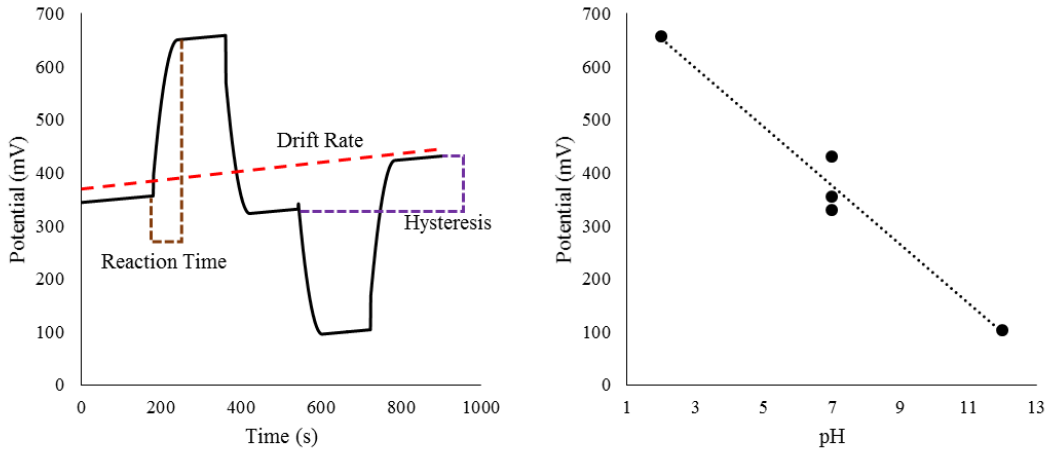

Figure 10 – Graphical example of a pH Data Loop, where pH is cycled form 7-2-7-12-7 (left), showing reaction time (brown), drift rate (red) and hysteresis (purple). A linear calibration plot is shown on the right. It should be noted that this data is an example only and is highly exaggerated, to clearly show drift, hysteresis and reaction time.

1.6 References

[1] S. Sörensen, Über die Messung und die Bedeutung der Wassorstoffionenkonzentration bei enzymatischen Prozessen, Carlsb. Lab. Kopenhagen. II (1909) 131–200.

[2] A. Rockwood, Meaning and Measurability of Single-Ion Activities, the Thermodynamic Foundations of pH, and the Gibbs Free Energy for the Transfer of Ions between Dissimilar Materials, ChemPhysChem. 16 (2015) 1978–1991. doi:10.1002/cphc.201500044.

[3] L. van de Velde, E. d'Angremont, W. Olthuis, Solid contact potassium selective electrodes for biomedical applications: a review, Talanta. 160 (2016) 56–65. doi:10.1016/j.talanta.2016.06.050.

[4] A. Cottrell, Introduction to Metallurgy, 2nd ed., Maney Publishing for IOM3, the institute of Materials, Minerals and Mining, 1975.

[5] A. Bhaqi, G. Chatwal, Environmental Chemistry, Global Media, 2009. https://ebookcentral.proquest.com/lib/ECU/detail.action?docID=3011337#.

[6] A. Conklin, Introduction to Soil Chemistry: Analysis and Instrumentation, Wiley and Sons, Incorperated, 2013. https://ebookcentral.proquest.com/lib/ECU/detail.action?docID=1584993#.

[7] D. Wang, Food Chemistry, Nova Science Publishers, 2012. https://ebookcentral.proquest.com/lib/ECU/detail.action?docID=3017667.

[8] P. Kurzweil, Metal Oxides and Ion-Exchanging Surfaces as pH Sensors in Liquids: State-of-the-Art and Outlook, Sensors. 9 (2009) 4955–4985. doi:10.3390/s90604955.

[9] D. Maurya, A. Sardarinejad, K. Alameh, Recent Developments in R.F. Magnetron Sputtered Thin Films for pH Sensing Applications—An Overview, Coatings. 4 (2014) 756–771. doi:10.3390/coatings4040756.

[10] N. Stradiotto, H. Yamanaka, M. Zanoni, Review Electrochemical Sensors : A Powerful Tool in Analytical Chemistry, J. Braz. Chem. Soc. 14 (2003) 159–173. doi:doi: 10.1590/S0103-50532003000200003.

[11] E. Bakker, P. Bühlmann, E. Pretsch, Polymer Membrane Ion-Selective Electrodes – What are the Limits?, Electroanalysis. 11 (1999) 915–933. doi:10.1002/(SICI)1521-4109(199909)11.

[12] E. Bakker, P. Buhlmann, E. Pretsch, The phase-boundary potential model, Talanta. 63 (2004) 3–20. doi:10.1016/j.talanta.2003.10.006.

[13] J. Hu, A. Stein, P. Bühlmann, Rational design of all-solid-state ion-selective electrodes and reference electrodes, TrAC Trends Anal. Chem. 76 (2016) 102–114. doi:10.1016/j.trac.2015.11.004.

[14] T. Cesar da Paixsao, Materials for Chemical Sensing., Springer (2016).

[15] S. Głąb, A. Hulanicki, G. Edwall, F. Folke, I. Ingman, W.F. Koch, Metal-Metal Oxide and Metal Oxide Electrodes as pH Sensors, Crit. Rev. Anal. Chem. 21 (1989) 29–47. doi:10.1080/10408348908048815.

[16] S. Głab, A. Hulanicki, G. Edwall, F. Ingman, Metal-Metal Oxide and Metal Oxide Electrodes as pH Sensors, Crit. Rev. Anal. Chem. 21 (1989) 29–47. doi:10.1080/10408348908048815.

[17] P. Chang, H. Chen, J. Ye, F. Sheu, J. Lu, Vertically aligned antimony nanowires as solid-state pH sensors, ChemPhysChem. 8 (2007) 57–61. doi:10.1002/cphc.200600514.

[18] A. Fog, R. Buck, Electronic semiconducting oxides as pH sensors, Sensors and Actuators. 5 (1984) 137–146. doi:10.1016/0250-6874(84)80004-9.

[19] I. Kolthhoff, B. Hartong, The antimony electrode as an indicator for hydrogen ions and its applciaiton on potetniometric titrations of acids and bases, Pharmac. Lab. Der Rijks Univ. (1924).

[20] K. Xu, X. Zhang, K. Hou, M. Geng, L. Zhao, The Effects of Antimony Thin Film Thickness on Antimony pH Electrode Coated with Nafion Membrane, J. Electrochem. Soc. 163 (2016) B417–B421. doi:10.1149/2.0191608jes.

[21] P. Salazar, F. Garcia-Garcia, F. Yubero, J. Gil-Rostra, A. González-Elipe, Characterization and application of a new pH sensor based on magnetron sputtered porous WO_3 thin films deposited at oblique angles, Electrochim. Acta. 193 (2016) 24–31. doi:10.1016/j.electacta.2016.02.040.

[22] C. Pan, J.C. Chou, T.P. Sun, S.K. Hsiung, Development of the tin oxide pH electrode by the sputtering method, Sensors Actuators, B Chem. 108 (2005) 863–869. doi:10.1016/j.snb.2004.11.033.

[23] N. Chou, J.C. Chou, T. Sun, S. Hsiung, Differential type solid-state urea biosensors based on ion-selective electrodes, Sensors Actuators, B Chem. 130 (2008) 359–366. doi:10.1016/j.snb.2007.09.014.

[24] K. Kreider, M. Tarlov, J. Cline, Sputtered thin-film pH electrodes of platinum, palladium, ruthenium, and iridium oxides, Sensors Actuators B. Chem. 28 (1995) 167–172. doi:10.1016/0925-4005(95)01655-4.

[25] W. Olthuis, M. Robben, P. Bergveld, M. Bos, W. Van Der Linden, pH Sensor Properties of Electrochemically Grown Iridium Oxide, Sensors Actuators B. 2 (1990) 247–256.

[26] S. Yao, M. Wang, M. Madou, A pH Electrode Based on Melt-Oxidized Iridium Oxide, J. Electrochem. Soc. 148 (2001) H29-H36. doi:10.1149/1.1353582.

[27] W. Huang, H. Cao, S. Deb, M. Chiao, J. Chiao, A flexible pH sensor based on the iridium oxide sensing film, Sensors Actuators A Phys. 169 (2011) 1–11. doi:10.1016/j.sna.2011.05.016.

[28] C. Nguyen, W. Huang, S. Rao, H. Cao, U. Tata, M. Chiao, J. Chiao, Sol-gel iridium oxide-based pH sensor array on flexible polyimide substrate, IEEE Sens. J. 13 (2013) 3857–3864. doi:10.1109/JSEN.2012.2236551.

[29] W. Olthuis, M. Robben, P. Bergveld, M. Bos, W. Van Der Linden, pH Sensor Properties of Electrochemically, Sensors Actuators B. 2 (1990) 247–256. doi:Doi 10.1016/0925-4005(90)80150-X.

[30] P. Steegstra, (2014) Hydrous iridium oxide for in situ pH sensing electrodeposition, properties and applications, University of Gothenburg, Sweden.

[31] T. Katsube, I. Lauks, J. Zemel, pH sensitive sputtered iridium oxide films, Sensors and Actuators. 2 (1982) 399–410.

[32] L. Kuo, Y. Chou, K. Chen, C. Lu, S. Chao, A precise pH microsensor using RF-sputtering IrO_2 and Ta_2O_5 films on Pt-electrode, Sensors Actuators, B Chem. 193 (2014) 687–691.

doi:10.1016/j.snb.2013.11.109.

[33] P. Kinlen, J. Heider, D. Hubbard, A solid-state pH sensor based on a Nafion-coated iridium oxide indicator electrode and a polymer-based silver chloride reference electrode, Sensors Actuators B Chem. 22 (1994) 13–25. doi:10.1016/0925-4005(94)01254-7.

[34] S. Carroll, R. Baldwin, Self-calibrating microfabricated iridium oxide pH electrode array for remote monitoring, Anal. Chem. 82 (2010) 878–885. doi:10.1021/ac9020374.

[35] M. Wang, S. Yao, M. Madou, A long-term stable iridium oxide pH electrode, Sensors Actuators, B Chem. 81 (2002) 313–315. doi:10.1016/S0925-4005(01)00972-8.

[36] H. Cao, V. Landge, U. Tata, Y. Seo, S. Rao, S. Tang, H. Tibbals, S. Spechler, J. Chiao, An implantable, batteryless, and wireless capsule with integrated impedance and pH sensors for gastroesophageal reflux monitoring, IEEE Trans. Biomed. Eng. 59 (2012) 3131–3139. doi:10.1109/TBME.2012.2214773.

[37] B. Zhou, C. Bian, J. Tong, S. Xia, Fabrication of a miniature multi-parameter sensor chip for water quality assessment, Sensors (Switzerland). 17 (2017) 1–14. doi:10.3390/s17010157.

[38] N. Uria, N. Abramova, A. Bratov, F. Munoz-Pascual, E. Baldrich, Miniaturized metal oxide pH sensors for bacteria detection, Talanta. 147 (2016) 364–369. doi:10.1016/j.talanta.2015.10.011.

[39] P. Kurzweil, Precious metal oxides for electrochemical energy converters: Pseudocapacitance and pH dependence of redox processes, J. Power Sources. 190 (2009) 189–200. doi:10.1016/j.jpowsour.2008.08.033.

[40] H. McMurray, P. Douglas, D. Abbot, Novel thick-film pH sensors based on ruthenium dioxide-glass composites, Sensors Actuators B. Chem. 28 (1995) 9–15. doi:10.1016/0925-4005(94)01536-Q.

[41] L. Manjakkal, K. Cvejin, J. Kulawik, K. Zaraska, D. Szwagierczak, G. Stojanovic, Sensing mechanism of RuO_2–SnO_2 thick film pH sensors studied by potentiometric method and electrochemical impedance spectroscopy, J. Electroanal. Chem. 759 (2015) 82–90. doi:10.1016/j.jelechem.2015.10.036.

[42] L. Manjakkal, K. Cvejin, J. Kulawik, K. Zaraska, D. Szwagierczak, R. Socha, Fabrication of thick film sensitive RuO_2-TiO_2 and Ag/AgCl/KCl reference electrodes and their application for pH measurements, Sensors Actuators, B Chem. 204 (2014) 57–67. doi:10.1016/j.snb.2014.07.067.

[43] J. Mihell, J. Atkinson, Planar thick-film pH electrodes based on ruthenium dioxide hydrate,

Sensors Actuators B Chem. 48 (1998) 505–511. doi:10.1016/S0925-4005(98)00090-2.

[44] K. Pasztor, A. Sekiguchi, N. Shimo, N. Kitamura, H. Masuhara, Electrochemically-deposited RuO_2 films as pH sensors, Sensors Actuators B. 14 (1993) 561–562.

[45] B. Xu, W. De Zhang, Modification of vertically aligned carbon nanotubes with RuO_2 for a solid-state pH sensor, Electrochim. Acta. 55 (2010) 2859–2864. doi:10.1016/j.electacta.2009.12.099.

[46] S. Zhuiykov, D. O'Brien, M. Best, Water quality assessment by an integrated multi-sensor based on semiconductor RuO_2 nanostructures, Meas. Sci. Technol. 20 (2009) 95201. doi:10.1088/0957-0233/20/9/095201.

[47] S. Zhuiykov, Morphology and sensing characteristics of nanostructured RuO_2 electrodes for integrated water quality monitoring sensors, Electrochem. Commun. 10 (2008) 839–843. doi:10.1016/j.elecom.2008.03.007.

[48] S. Zhuiykov, Morphology of Pt-doped nanofabricated RuO_2 sensing electrodes and their properties in water quality monitoring sensors, Sensors Actuators, B Chem. 136 (2009) 248–256. doi:10.1016/j.snb.2008.10.030.

[49] L. Bousse, N. De Rood, P. Bergveld, Operation of Chemically Sensitive Field-Effect Sensors As a Function of the Insulator-Electrolyte Interface, IEEE Trans. Electron Devices. 30 (1983) 1263–1270. doi:10.1109/T-ED.1983.21284.

[50] S. Zhuiykov, E. Kats, V. Plashnitsa, N. Miura, Toward selective electrochemical "e-tongue": Potentiometric DO sensor based on sub-micron ZnO-RuO_2 sensing electrode, Electrochim. Acta. 56 (2011) 5435–5442. doi:10.1016/j.electacta.2011.01.062.

[51] S. Zhuiykov, E. Kats, M. Breedon, N. Miura, The influence of Cu_2O - doped RuO_2 electrode thickness on the sensig performance of planar electrochemical pH sensors, Mater. Lett. 75 (2012) 165–168. doi:10.1016/j.matlet.2012.01.107.

[52] J. Yi-Hung Liaoa, Preparation and characteristics of ruthenium dioxide for pH array sensors with real-time measurement system, Sensors Actuators B Chem. 128 (2008) 603–612. doi:10.1109/ICSENS.2012.6411062.

[53] Y. Liao, J. Chou, Potentiometric Multisensor Based on Ruthenium Dioxide Thin Film With a Bluetooth Wireless and Web-Based Remote Measurement System, IEEE Sens. J. 9 (2009) 1887–1894. doi:10.1109/JSEN.2009.2031563.

[54] J. Chou, W. Hsia, Study on the characteristics of the measurement system for pH array sensors, Int. J. Chem. Biol. 3 (2009) 308–311. http://www.waset.org/publications/10246.

[55] M. Brischwein, H. Grothe, J. Wiest, M. Zottmann, J. Ressler, B. Wolf, Planar Ruthenium Oxide Sensors for Cell-on-a-Chip Metabolic Studies, Chem. Analityczna. 54 (2009) 1193–1201. http://cat.inist.fr/?aModele=afficheN&cpsidt=22644344.

[56] M. Kahram, M. Asnavandi, A. Dolati, Synthesis and electrochemical characterization of sol–gel-derived RuO_2/carbon nanotube composites, J. Solid State Electrochem. 18 (2013) 993–1003. doi:10.1007/s10008-013-2346-2.

[57] J. Chou, J. Chen, Y. Liao, J. Chen, C. Lin, J. Lin, C. Jhang, R. Chen, Fabrication and characteristic analysis of a remote real-time monitoring applied to glucose sensor system based on microfluidic framework, IEEE Sens. J. 15 (2015) 3234–3240. doi:10.1109/JSEN.2015.2407910.

[58] L. Manjakkal, K. Cvejin, J. Kulawik, K. Zaraska, D. Szwagierczak, A Low-Cost pH Sensor Based on RuO_2 Resistor Material, Nano Hybrids. 5 (2013) 1–15. doi:10.4028/www.scientific.net/NH.5.1.

[59] L. Manjakkal, K. Cvejin, J. Kulawik, K. Zaraska, D. Szwagierczak, K. Division, Electrochemical Interdigitated Conductimetric pH Sensor Based on RuO_2 Thick Film Sensitive Layer, in: Int. Conf. Expo. Lectrical Power Eng., 2014: pp. 797–800.

[60] L. Manjakkal, K. Cvejin, J. Kulawik, K. Zaraska, R.P. Socha, D. Szwagierczak, X-ray photoelectron spectroscopic and electrochemical impedance spectroscopic analysis of RuO_2-Ta_2O_5 thick film pH sensors, Anal. Chim. Acta. 931 (2016) 47–56. doi:10.1016/j.aca.2016.05.012.

[61] L. Manjakkal, B. Synkiewicz, K. Zaraska, K. Cvejin, J. Kulawik, D. Szwagierczak, Development and characterization of miniaturized LTCC pH sensors with RuO_2 based sensing electrodes, Sensors Actuators B Chem. 223 (2016) 641–649. doi:10.1016/j.snb.2015.09.135.

[62] L. Manjakkal, K. Zaraska, K. Cvejin, J. Kulawik, D. Szwagierczak, Potentiometric RuO_2–Ta_2O_5 pH sensors fabricated using thick film and LTCC technologies, Talanta. 147 (2016) 233–240. doi:10.1016/j.talanta.2015.09.069.

[63] D. Maurya, A. Sardarinejad, K. Alameh, High-sensitivity pH sensor employing a sub-micron ruthenium oxide thin-film in conjunction with a thick reference electrode, Sensors Actuators, A Phys. 203 (2013) 300–303. doi:10.1016/j.sna.2013.09.003.

[64] A. Sardarinejad, D. Maurya, K. Alameh, The effects of sensing electrode thickness on ruthenium oxide thin-film pH sensor, Sensors Actuators, A Phys. 214 (2014) 15–19. doi:10.1016/j.sna.2014.04.007.

[65] A. Sardarinejad, D. Maurya, K. Alameh, The pH Sensing Properties of RF Sputtered RuO_2 Thin-Film Prepared Using Different Ar/O2 Flow Ratio, Materials (Basel). 8 (2015) 3352–3363. doi:10.3390/ma8063352.

[66] A. Sardarinejad, D. Maurya, M. Khaled, K. Alameh, Temperature effects on the performance of RuO_2 thin-film pH sensor, Sensors Actuators A Phys. 233 (2015) 414–421. doi:10.1016/j.sna.2015.07.027.

[67] D. Maurya, A. Sardarinejad, K. Alameh, Ruthenium oxide ion selective thin-film electrodes for engine oil acidity monitoring, Meas. Sci. Technol. 26 (2015) 65102. doi:10.1088/0957-0233/26/6/065102.

[68] L. Bousse, H. van den Vlekkert, N. de Rooij, Hysteresis in $A1_2O_3$ -gate ISFETs, Sensors Actuators B Chem. 2 (1990) 103–110. doi:10.1016/0925-4005(90)80018-U.

[69] L. Bousse, The role of buried OH sites in the response mechanism of inorganic pH sensitive ISFETs, 6 (1984) 65–78.

[70] N. Bahari, A. Zain, A. Abdullah, D. Sheng, M. Othman, Study on pH sensing properties of RF magnetron sputtered tantalum pentoxide (Ta_2O_5) thin film, 2010 IEEE Int. Conf. Semicond. Electron. (2010) 76–78. doi:10.1109/SMELEC.2010.5549429.

[71] T. Akiyama, Y. Ujihira, Y. Okabe, Ion-sensitive field-effect transistors with inorganic gate oxide for pH sensing, IEEE Trans. Electron Devices. 29 (1982) 1936–1941. doi:10.1109/T-ED.1982.21054.

[72] Q. Zhang, W. Liu, C. Sun, H. Zhang, W. Pang, On-chip surface modified nanostructured ZnO as functional pH sensors, Nanotechnology. 26 (2015) 355202. doi:10.1088/0957-4484/26/35/355202.

[73] C. Lai, C.M. Yang, T. Lu, Thickness effects on pH response of HfO_2 sensing dielectric improved by rapid thermal annealing, Japanese J. Appl. Physics, Part 1 Regul. Pap. Short Notes Rev. Pap. 45 (2006) 3807–3810. doi:10.1143/JJAP.45.3807.

[74] P. Em, ISFET , Theory and Practice, in: IEEE Sensors Conf. Toronto, 2003: pp. 1–26.

[75] F. Yue, T. Ngin, G. Hailin, A novel paper pH sensor based on polypyrrole, Sensors Actuators, B Chem. 32 (1996) 33–39. doi:10.1016/0925-4005(96)80106-7.

[76] W. Prissanaroon-Ouajai, P. James Pigram, A. Sirivat, Simple Solid-state Ag/AgCl Reference Electrode and Its Integration with Conducting Polypyrrole Electrode for the Production of All-solid-state pH Sensor, KMUTNB Int. J. Appl. Sci. Technol. (2016) 1–9. doi:10.14416/j.ijast.2016.05.001.

[77] T. Lindfors, A. Ivaska, pH sensitivity of polyaniline and its substituted derivatives, J. Electroanal. Chem. 531 (2002) 43–52. doi:10.1016/S0022-0728(02)01005-7.

[78] J. Yoon, S. Hong, S. Yun, S. Lee, T. Lee, K. Lee, B. Choi, High performance flexible pH sensor based on polyaniline nanopillar array electrode, J. Colloid Interface Sci. 490 (2017) 53–58. doi:10.1016/j.jcis.2016.11.033.

[79] M. Liu, Y. Ma, L. Su, K. Chou, X. Hou, A titanium nitride nanotube array for potentiometric sensing of pH, Analyst. 141 (2016) 1693–1699. doi:10.1039/C5AN02675J.

[80] C. Li, K. Han, X. Pham, G. Seong, A single-walled carbon nanotube thin film-based pH-sensing microfluidic chip, Analyst. 139 (2014) 2011-2015. doi:10.1039/c3an02195e.

[81] P. Buhlmann, L. Chen, Ion-Selective Electrodes With Ionophore-Doped Sensing Membranes, 2011-2015. doi:ISBN: 978-0-470-74640-0.

[82] E. Bakker, E. Pretsch, Potentiometric Determination of Effective Complex Formation Constants of Lipophilic Ion Carriers within Ion-Selective Electrode Membranes, J. Electrochem. Soc. 144 (1997) L125–L127. doi:Doi 10.1149/1.1837633.

[83] J. Hu, K. Ho, X. Zou, W. Smyrl, A. Stein, P. Buhlmann, All-solid-state reference electrodes based on colloid-imprinted mesoporous carbon and their application in disposable paper-based potentiometric sensing devices, Anal. Chem. 87 (2015) 2981–2987. doi:10.1021/ac504556s.

[84] S. Anastasova-Ivanova, U. Mattinen, A. Radu, J. Bobacka, A. Lewenstam, J. Migdalski, M. Danielewski, D. Diamond, Development of miniature all-solid-state potentiometric sensing system, Sensors Actuators, B Chem. 146 (2010) 199–205. doi:10.1016/j.snb.2010.02.044.

[85] M. Shinwari, D. Zhitomirsky, I. Deen, P. Selvaganapathy, M. Deen, D. Landheer, Microfabricated Reference Electrodes and their Biosensing Applications, Sensors. 10 (2010) 1679–1715. doi:10.3390/s100301679.

[86] M. Glanc, M. Sophocleous, J. Atkinson, E. Garcia-Breijo, The effect on performance of fabrication parameter variations of thick-film screen printed silver/silver chloride potentiometric reference electrodes, Sensors Actuators, A Phys. 197 (2013) 1–8. doi:10.1016/j.sna.2013.03.036.

[87] T. Kim, S. Hong, S. Yang, A Solid-State Thin-Film Ag/AgCl Reference Electrode Coated with Graphene Oxide and Its Use in a pH Sensor, Sensors. 15 (2015) 6469–6482. doi:10.3390/s150306469.

[88] D. Moschou, T. Trantidou, A. Regoutz, D. Carta, H. Morgan, T. Prodromakis, Surface and Electrical Characterization of Ag/AgCl Pseudo-Reference Electrodes Manufactured with

Commercially Available PCB Technologies, Sensors. 15 (2015) 18102–18113. doi:10.3390/s150818102.

[89] P. Brewer, R. Leese, R. Brown, An improved approach for fabricating Ag/AgCl reference electrodes, Electrochim. Acta. 71 (2012) 252–257. doi:10.1016/j.electacta.2012.03.164.

[90] D. Stoica, P. Brewer, R. Brown, P. Fisicaro, Influence of fabrication procedure on the electrochemical performance of Ag/AgCl reference electrodes, Electrochim. Acta. 56 (2011) 10009–10015. doi:10.1016/j.electacta.2011.08.089.

[91] P. Brewer, A. Leach, R. Brown, The Role of the Electrolyte in the Fabrication of Ag|AgCl Reference Electrodes for pH Measurement, Electrochim. Acta. 161 (2015) 80–83. doi:10.1016/j.electacta.2015.02.066.

[92] A. Cranny, N. Harris, M. Nie, J. Wharton, R. Wood, K. Stokes, Screen-printed potentiometric Ag/AgCl chloride sensors: Lifetime performance and their use in soil salt measurements, Sensors Actuators, A Phys. 169 (2011) 288–294. doi:10.1016/j.sna.2011.01.016.

[93] W. Liao, T. Chou, Fabrication of a Planar-Form Screen-Printed Solid Electrolyte Modified Ag / AgCl Reference Electrode for Application in a Potentiometric Biosensor Fabrication of a Planar-Form Screen-Printed Solid Electrolyte Modified Ag / AgCl Reference Electrode for App, Anal. Chem. 78 (2006) 4219–4223. doi:10.1021/ac051562.

[94] N. Kwon, K. Lee, M. Won, Y. Shim, An all-solid-state reference electrode based on the layer-by-layer polymer coating, Analyst. 132 (2007) 906-912. doi:10.1039/b706905g.

[95] M. Sophocleous, M. Glanc-Gostkiewicz, J. Atkinson, E. Garcia-Breijo, An experimental analysis of Thick-Film solid-state reference electrodes, in: Proc. IEEE Sensors, 2012: pp. 12–15. doi:10.1109/ICSENS.2012.6411137.

[96] Z. Mousavi, K. Granholm, T. Sokalski, A. Lewenstam, An analytical quality solid-state composite reference electrode., Analyst. 138 (2013) 5216–20. doi:10.1039/c3an00852e.

[97] Ł. Tymecki, E. Zwierkowska, R. Koncki, Screen-printed reference electrodes for potentiometric measurements, Anal. Chim. Acta. 526 (2004) 3–11. doi:10.1016/j.aca.2004.08.056.

[98] J. Atkinson, M. Glanc, P. Boltryk, M. Sophocleous, E. Garcia-Breijo, An investigation into the effect of fabrication parameter variation on the characteristics of screen printed thick film silver/silver chloride reference electrodes, Microelectron. Int. 28 (2011) 49–53. doi:10.1108/13565361111127368.

[99] D. Patrick J. Kinlen, John E. Heider, A solid-state pH sensor based on a Nafion-coated iridium

oxide indicator electrode and a polymer-based silver chloride reference electrode, Sensors Actuators B Chem. 22 (1994) 13–25. doi:doi:10.1016/0925-4005(94)01254-7.

[100] I. Shitanda, M. Komoda, Y. Hoshi, M. Itagaki, An instantly usable paper-based screen-printed solid-state KCl/Ag/AgCl reference electrode with long-term stability, Analyst. 140 (2015) 6481–6484. doi:10.1039/C5AN00617A.

[101] I. Shitanda, H. Kiryu, M. Itagaki, Improvement in the long-term stability of screen-printed planar type solid-state Ag/AgCl reference electrode by introducing poly(dimethylsiloxane) liquid junction, Electrochim. Acta. 58 (2011) 528–531. doi:10.1016/j.electacta.2011.09.086.

[102] T. Guinovart, G. Crespo, F. Rius, F. Andrade, A reference electrode based on polyvinyl butyral (PVB) polymer for decentralized chemical measurements., Anal. Chim. Acta. 821 (2014) 72–80. doi:10.1016/j.aca.2014.02.028.

[103] T. Guinovart, G. Valdés-Ramírez, J. Windmiller, F. Andrade, J. Wang, Bandage-Based Wearable Potentiometric Sensor for Monitoring Wound pH, Electroanalysis. 26 (2014) 1345–1353. doi:10.1002/elan.201300558.

[104] T. Guinovart, A. Bandodkar, J. Windmiller, F. Andrade, J. Wang, A potentiometric tattoo sensor for monitoring ammonium in sweat., Analyst. 138 (2013) 7031–8. doi:10.1039/c3an01672b.

[105] M. Parrilla, J. Ferre, T. Guinovart, F. Andrade, Wearable Potentiometric Sensors Based on Commercial Carbon Fibres for Monitoring Sodium in Sweat, Electroanalysis. (2016) 1267–1275. doi:10.1002/elan.201600070.

[106] A. Kisiel, K. Kijewska, M. Mazur, K. Maksymiuk, A. Michalska, Polypyrrole Microcapsules in All-solid-state Reference Electrodes, Electroanalysis. 24 (2012) 165–172. doi:10.1002/elan.201100551.

[107] C. Duarte-Guevara, V. Swaminathan, M. Burgess, B. Reddy, E. Salm, Y. Liu, J. Rodriguez-Lopez, R. Bashir, On-chip metal/polypyrrole quasi-reference electrodes for robust ISFET operation, Analyst. 140 (2015) 3630–3641. doi:10.1039/C5AN00085H.

[108] A. Kisiel, H. Marcisz, A. Michalska, K. Maksymiuk, All-solid-state reference electrodes based on conducting polymers., Analyst. 130 (2005) 1655–1662. doi:10.1039/b510868c.

[109] J. Noh, S. Park, H. Boo, H. Kim, T. Chung, Nanoporous platinum solid-state reference electrode with layer-by-layer polyelectrolyte junction for pH sensing chip., Lab Chip. 11 (2011) 664–71. doi:10.1039/c0lc00293c.

[110] E. Bakker, Hydrophobic Membranes as Liquid Junction-Free Reference Electrodes,

Electroanalysis. 11 (1999) 788–792. doi:10.1002/(SICI)1521-4109(199907)11:10/11<788::AID-ELAN788>3.0.CO;2-4.

[111] T. Zhang, C.Z. Lai, M.A. Fierke, A. Stein, P. Buhlmann, Advantages and limitations of reference electrodes with an ionic liquid junction and three-dimensionally ordered macroporous carbon as solid contact, Anal. Chem. 84 (2012) 7771–7778. doi:10.1021/ac3011507.

Chapter 2 of this thesis is currently not available in this version of the thesis.

This chapter has been published as:

W. Lonsdale, D.K. Maurya, M. Wajrak, K. Alameh, Effect of ordered mesoporous carbon contact layer on the sensing performance of sputtered RuO2 thin film pH sensor, Talanta. 164 (2017) 52–56. doi:10.1016/j.talanta.2016.11.020

Chapter 3 of this thesis is currently not available in this version of the thesis.

This chapter has been published as:

W. Lonsdale, M. Wajrak, K. Alameh, Effect of conditioning protocol, redox species and material thickness on the pH sensitivity and hysteresis of sputtered RuO2 electrodes, Sensors Actuators B Chem. 252 (2017) 251–256. doi:10.1016/j.snb.2017.05.171

Chapter 4 – RuO_2 pH Sensor with Super-Glue-Inspired Reference Electrode

This chapter was published as an article in the journal MDPI Sensors, 2017, vol.17, pp 2036. This article appears as it does in print, with the exception of minor changes to the layout, number formats, font size and font style, which was implemented to maintain consistency in the formatting of this thesis.

4.1 Abstract

A pH-sensitive RuO_2 electrode coated in a commercial cyanoacrylate adhesive typically exhibits very low pH sensitivity, and could be paired with a RuO_2 working electrode as a differential type pH sensor. However, such sensors display poor performance in real sample matrices. A pH sensor employing a RuO_2 pH-sensitive working electrode and a SiO_2-PVB junction-modified RuO_2 reference electrode is developed as an alternative high-performance solution. This sensor exhibits a performance similar to that of a commercial glass pH sensor in some common sample matrices, particularly, an excellent pH sensitivity of 55.7 mV/pH, a hysteresis as low as 2.7 mV, and a drift below 2.2 mV/h. The developed sensor structure opens the way towards the development of a simple, cost effective, and robust pH sensor for pH analysis in various sample matrices.

Keywords: ruthenium oxide; solid-state pH sensor; polyvinyl butyral; silicon dioxide; differential-type pH sensor

4.2 Background

The use of RuO_2 films for the manufacture of solid state potentiometric pH sensors has several advantages, namely Nernstian pH sensitivity, insolubility over a wide pH range, good reproducibility, low hysteresis, and reduced cost (in comparison to the more commonly studied IrO_2 films) [1–4]. The pH sensing properties of RuO_2 films have been reported by numerous groups [5–7]. Briefly, RuO_2 undergoes the following redox reaction:

$$\mathrm{RuO}_x(\mathrm{OH})_y + \mathrm{ze}^- + \mathrm{zH}^+ \leftrightarrow \mathrm{RuO}_{x-y}(\mathrm{OH})_{y+z} \quad (1)$$

where the electrode's potential, *E*, in mV and at 22 °C, is given by the Nernst equation, which simplifies to:

$$E = E^0 - 58.6\mathrm{pH} \quad (2)$$

Radio frequency magnetron sputtering (RFMS) is a convenient technique for the deposition of thin films with well-controlled thickness and stoichiometry [8]. This technique is therefore attractive for the development of RuO_2 pH sensors featuring high purity and reproducible performance.

Metal oxide pH sensors are commonly paired with quasi Ag|AgCl reference electrodes for potentiometry, since they are simple to construct [9–11]. However, quasi reference electrodes are not always suitable for application in samples due to their cross sensitivities. For example, an Ag|AgCl electrode is sensitive to the concentration of Cl^- ions in solution, according to the following equations:

$$AgCl_{(s)} + e^- \leftrightarrow Ag_{(s)} + Cl^-_{(aq)} \tag{3}$$

$$E = E^0 + \left(\frac{RT}{nF}\right)\ln[\alpha_{Cl^-}] + \left(\frac{RT}{nF}\right)\ln\frac{[AgCl]}{[Ag]} \tag{4}$$

$$E = E^0 + 58.6p[Cl] \tag{5}$$

where *R*, *T*, *n*, and *F* are the universal gas constant, temperature, number of electrons, and Faraday constant, respectively. This makes such sensors difficult to use in sample solutions, where Cl^- concentration changes. Much research has been undertaken to develop Cl^--insensitive solid-state reference electrodes [12–14]. This is commonly achieved by adding a KCl electrolyte layer to the Ag|AgCl electrode, which results in a high concentration of Cl^- at the electrode's surface and thus a stable electrode potential. KCl is used to minimize the formation of a liquid junction potential, due to the nearly equal ionic mobilities of K^+ and Cl^- [15].

Previously, authors have reported numerous electrolyte layers and modification procedures including gels [16], fused ceramics/glasses [17,18], and other polymers [19,20]. Typically, gels suffer from short life spans and are not commonly used due to their low melting points, whilst fused glass requires high temperatures during their manufacture process. This makes polymers more attractive, since they can be drop-cast and dried at room temperature. However, polymers are more chemically reactive than glass and can be prone to interference from solvents and other agents. Electrodes based on KCl electrolyte layers also have varying lifespans depending on the rate at which KCl leaches from the electrode. Lifespans ranging from several days [15] to several months [21] have been reported.

Other approaches for the development of solid-state pH sensor reference electrodes include the use of bronzes or similar materials that have low pH sensitivity [22,23]. However, these kinds of sensors typically exhibit poor performance due to high hysteresis, drifts, and instability caused by the reference electrode. Another approach involves modifying the pH-sensitive working electrode, so that the pH, and therefore the potential at the electrode's surface, is constant [24]. J. Noh et al. [25] reported one such differential pH sensor based on a complex series of polymer layers over a Pt

electrode. In this paper, a differential-type pH sensor, employing RuO_2 as a pH-sensitive working electrode and RuO_2 modified with a simple polymer layer loaded with silica as a reference electrode, is proposed and its performance is investigated experimentally.

4.3 Preliminary Work

In this study, a RuO_2 electrode was covered with a commercial adhesive (Loctite Super Glue—Gel Control) and, surprisingly, it showed very low pH sensitivity, so it was investigated for use as a reference electrode. However, the manufacture of this electrode was difficult to replicate. The initial electrode was manufactured on a Zensor screen-printed carbon electrode on a polyethylene terephthalate (PET) substrate, with a 500-nm thick RuO_2 film. A 1–2 mm layer of the glue was applied over the RuO_2 working area, and the glue was cured by placing it in a pH 7 buffer solution for 24 h. Curing in the pH 7 buffer solution was found to be essential, as a voltage reading could not be obtained for electrodes that were cured in air, indicating that a complete water tight encapsulation layer had formed over the RuO_2 film. When cured in pH 7 buffer, an opaque white material was formed (when the electrode was dry), which quickly became clear when submerged in a liquid. This indicated that the glue cured at pH 7 possessed a porous structure. Presumably, the formation of this porous material can be attributed to the curing process, since cyanoacrylate (superglue) polymerizes when exposed to H_2O. This likely results in rapid polymerization (and a porous structure) when the glue is cured in a solution, whereas in air the glue is able to cure slowly, forming a smooth clear-plastic layer. Figure 1 shows SEM images of the air-cured and pH 7-cured super-glue surfaces. It is obvious from Figure 1 that the air-cured glue is flatter and more uniform compared to the pH 7-cured glue, which is rough and appears to have many pores, when viewed at the same magnification.

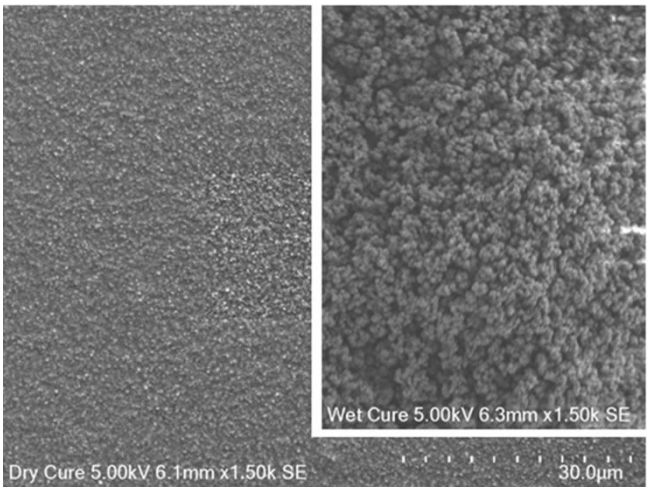

Figure 1 – Surfaces of air-cured and pH 7-cured super-glue (inset), at the same magnification.

Replication of this electrode using DropSens ordered meso-porous carbon (OMC) substrates with 500 nm of RuO_2 resulted in electrodes with inconsistent performance. It was noted that the Zensor-based

electrode was more opaque when dried and became clear faster when hydrated, compared to the OMC electrodes. Closer examination of the Zensor electrodes when applying the glue revealed that there was an unknown chemical reaction occurring between the electrical isolation layer and the super glue, which seemed to result in a more porous structure. Zensor substrates were electrically isolated using a material that dissolved in acetone, whilst the DropSens electrodes used a solvent-resistant resin.

When paired with a RuO_2 working electrode, the original Zensor electrode performed well in pH buffer solutions (results shown in the following sections). However, when applied to real sample matrices, the sensor gave inaccurate results due to large shifts in potential and instability. The reason for this was not investigated; however, it could be due to the formation of an undefined liquid junction potential caused by unknown compounds in the proprietary products used in its construction. Therefore, research was undertaken to replicate this type of differential reference electrode, but using known components.

A possible explanation for the pH insensitivity caused by the superglue layer could be that the cyanoacrylate acts as a porous structure, allowing a small volume of liquid to penetrate to the RuO_2 surface, and the fumed silica added to thicken the glue into a gel acts as a reservoir of H^+/OH^- ions, due to their adsorption on the SiO_2 surface [26]. This reservoir is able to buffer the small volume of liquid that fills the porous cyanoacrylate, resulting in a relatively stable pH and thus potential at the RuO_2 surface.

T. Guinovart et al. [27–29] reported a reference electrode that consists of a Polyvinyl Butyral (PVB) layer loaded with NaCl on an Ag|AgCl electrode. When conditioned in 3 M KCl, a nano-porous structure develops, which controls the flow of NaCl from the electrode. This results in a stable electrode potential due a controlled Cl^- concentration at the Ag|AgCl surface, with low liquid junction potential. Their electrodes exhibited good stability and lifetime, but were prone to some pH sensitivity below pH 4. Here, PVB was used to create a porous junction loaded with finely ground SiO_2. When placed over a RuO_2 electrode, this junction resulted in relatively stable potential between pH 1.5 and 12. When paired with a RuO_2 working electrode, this differential-type pH sensor exhibited a performance comparable to a commercial glass pH sensor in some common sample matrices.

4.4 Method

4.4.1 Working Electrode Fabrication

Several pH-sensitive working electrodes were manufactured, as previously reported in reference [30], with the exception that in this work RuO_2 thickness was only 500 nm. Amorphous thin-films of RuO_2 were obtained by RFMS deposition at room temperature onto 4-mm diameter OMC contacts of Dropsens (DRP-110OMC) electrodes, isolated via shadow masking. RuO_2 was deposited from a RuO_2 target (99.95% purity) using 100 W sputter power with an 80:20 $Ar:O_2$ process gas ratio at 1 mTorr chamber pressure.

4.4.2 Reference Electrode Fabrication

The pH-insensitive reference electrodes were manufactured by sputtering either 500 nm of RuO_2 or 500 nm of Ag using the procedure as above; however, Ag was sputtered from an Ag target (99.99% purity) using 70 W sputter power in an Ar plasma at 1 mTorr chamber pressure. A well was created around each electrode working area by gluing (Loctite Super Glue—Gel Control) an acrylic ring (5 mm internal diameter, 7 mm outside diameter, 5 mm height) that was made using a laser cutter/engraver. Once the glue had completely dried, silver electrodes were chlorinated with 50 mM $FeCl_3$, until a uniform brown AgCl layer had formed; meanwhile, RuO_2 electrodes were hydrated in pH 7 buffer for 48 h. The silver electrode-wells were filled with 50 mg of KCl and then topped with a total of 250 µL of PVB^{NaCl} solution over three aliquots, electrodes were allowed to dry overnight between each addition. The RuO_2 electrode-wells were filled with either 50 mg of ground SiO_2 and topped with a total of 250 µl of PVB^{Sio2} solution, or with 25 mg of ground SiO_2, 25 mg of KCl and topped with 250 µL of $PVB^{Sio2+KCl}$ solution. PVB solutions were prepared by mixing the reagents shown in Table 1, together in a sealed vial, after which they were homogenized using an ultrasonic bath until uniform (approximately 30 min). This resulted in three different electrode types, namely, AgCl-KCl, RuO_2-SiO_2, and RuO_2-SiO_2-KCl, along with one glued-RuO_2 reference electrode, which consisted of 500 nm RuO_2 on a Zensor screen-printed carbon electrode coated in Loctite Super Glue—Gel Control and cured in pH 7 buffer for 24 h, as well as a quasi Ag|AgCl electrode.

Table 1 – Composition of the different polyvinyl butyral (PVB) solutions.

Solution	Methanol (mL)	PVB (mg)	NaCl (mg)	KCl (mg)	SiO_2 (mg)
PVB^{NaCl}	2.0	234	150	-	-
PVB^{Sio2}	2.0	234	-	-	150
$PVB^{Sio2+KCl}$	2.0	234	-	150	150

4.4.3 Potentiometric Measurements

A Keysight Technologies (Santa Rosa, USA) 34410A digital multimeter was used to record the potential between the working and reference electrodes [8]. The potential was recorded for 180 s at 1 s intervals using number of power line cycles (NPLC) set to 1, operating in the High-Impedance mode. For calculations, the last 30 data points were averaged from each potential recording to produce individual measurements (this avoided the rapid shift that typically occurs during the first 30 s of recording due to electrode equilibration). These measurements were then used to calculate the sensitivity, E^0, hysteresis, and drift of the sensors [10]. The hysteresis was calculated using the difference between consecutive measurements at pH 12 [30], while electrode drift was calculated using the slope of the line-of-best-fit for the data at pH 12 over the measurement period [30]. Electrode reaction time was defined as the time taken to reach within 3 mV (i.e., 0.05 pH) of the stable potential. All measurements were made in triplicate at 22 °C in commercial pH buffers (Rowe Scientific) and error bars represent the 95% confidence intervals.

4.5 Results and Discussion

4.5.1 Reference Electrode Performance

All RuO_2 electrodes were conditioned in pH 7 buffer for 24 h before use; the AgCl-KCl electrode was conditioned in 3 M KCl for 24 h before use; and the Quasi-Ag-AgCl electrode was conditioned in pH 7 buffer for 5 min before use (to prevent loss of AgCl). The pH and KCl sensitivity for each of the manufactured electrodes was examined by recording their responses against a commercial glass double junction Ag|AgCl|KCl reference electrode (Sigma). A summary of approximate pH and KCl sensitivity values for the manufactured electrodes is shown in Table 2. Figure 2 shows pH and KCl sensitivities of the manufactured electrodes. It is obvious from Table 2 and Figure 2 that all electrodes, apart from the Quasi-Ag|AgCl, exhibit low pH sensitivity between pH 1 and 12, compared to the RuO_2 electrode, and that all electrodes apart from the Quasi-Ag|AgCl exhibit a relatively low response to KCl concentration. It should be noted that the non-linear pH response observed for the Quasi-Ag|AgCl electrode could be due to changes in chloride concentration between the commercial pH buffers used. In contrast, the sensitivity of the RuO_2-junction electrodes could be due to an inherent liquid junction potential, due to the junction material. These results show that, apart from Quasi-Ag|AgCl, all reference electrodes manufactured here could potentially be paired with a RuO_2 working electrode for the development of an accurate pH sensor.

Table 2 – Summary of approximate pH and KCl sensitivity values for the manufactured electrodes. Electrode names are color coded to match their respective data series in Figure 2.

Electrode	pH Sensitivity		KCl Sensitivity	
	mV/pH	R^2	mV/pKCl	R^2
RuO_2	−57	0.999	−6.7	0.629
RuO_2-SiO_2	−1.5	0.304	0.9	0.020
RuO_2-SiO_2-KCl	−4.5	0.967	2.4	0.118
Glued-RuO_2	−1.7	0.523	−2.3	0.178
Quasi-Ag|AgCl	14	0.557	43	0.964
AgCl-KCl	0.5	0.823	5.2	0.984

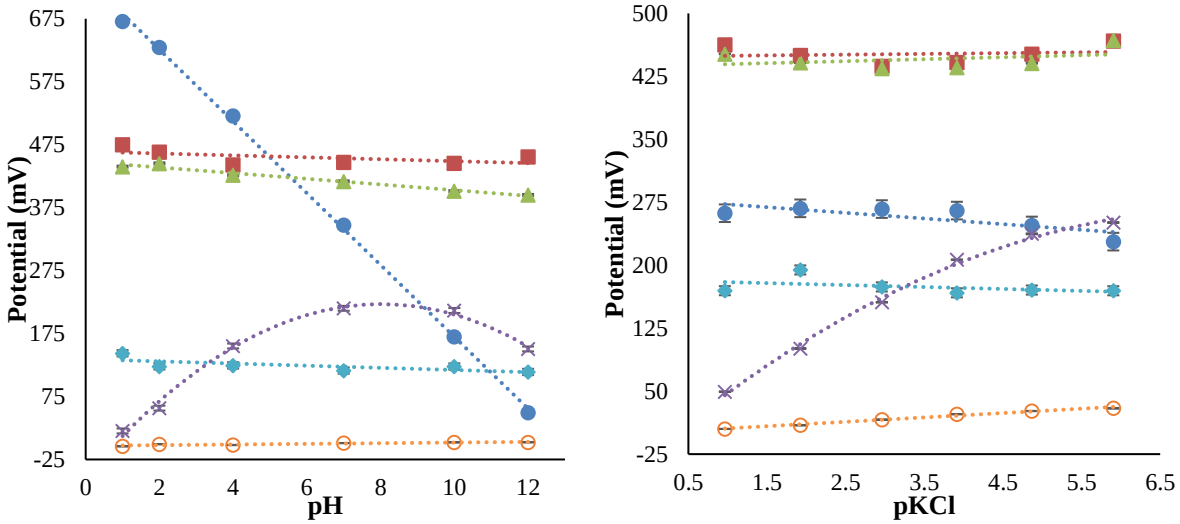

Figure 2 – pH (left) and KCl (right) sensitivity of manufactured electrodes; 500 nm RuO_2 (Blue Dots), RuO_2-SiO_2 (Red Squares), RuO_2-SiO_2-KCl (Green Triangles), Glued-RuO_2 (Aqua Diamonds), Quasi-AgCl (Purple Crosses), and AgCl-KCl (Orange Circles).

4.5.2 pH Sensor Performance

Due to their low sensitivities to pH and KCl, the Glued-RuO_2, RuO_2-SiO_2, RuO_2-SiO_2-KCl, and AgCl-KCl electrodes were paired with a RuO_2 working electrode, giving four pH sensors. The effect of ageing, drift, and hysteresis were minimized by conditioning the sensors in a pH 7 buffer overnight, then equilibrating in a pH 12 buffer for 1 h before use [7]. The pH sensitivity, E^0, linearity, hysteresis, and drift of these sensors was then examined by measuring sensor response when looped from pH 12–10–7–4–2–1.5 three times, with pH 12 between each step. Each pH data loop is presented individually in Figure 3, whilst the pH sensing properties are summarized in Table 3.

Table 3 – Summary of pH sensor performance calculated from pH loop data.

Reference Electrode	Sensitivity (mV/pH)		E^0 (mV)		R^2	Hysteresis (mV)		Drift (mV/h)
Glued-RuO_2	−56.2	±0.5	483	±7.3	0.9988	2.1	±0.7	28
RuO_2-SiO_2	−55.7	±0.6	160	±1.4	0.9980	2.7	±1.0	2.2
RuO_2-SiO_2-KCl	−52.8	±0.2	143	±0.5	0.9980	1.4	±0.7	7.6
AgCl-KCl	−58.1	±1.6	620	±19	0.9996	6.7	±2.4	31

The sensor employing an AgCl-KCl reference electrode exhibited the highest sensitivity (58.1 mV/pH), which is close to the theoretical maximum of 58.6 mV/pH, and agrees with previously reported results for this type of RuO_2 working electrode against a glass double junction Ag|AgCl|KCl reference electrode [30]. However, the potential drifted during individual pH readings for this sensor, resulting in higher hysteresis and a larger drift over the experimental period. The sensors employing RuO_2-SiO_2 and RuO_2-SiO_2-KCl-based reference electrodes exhibited lower sensitivities to pH than the AgCl-KCl-based sensor. However, such sensors exhibited short reaction times (<30 s) (as shown in Figure 3) and a higher degree of stability, resulting in much lower hysteresis and drift values. The Glued-RuO_2 pH sensor showed comparable results to the RuO_2-SiO_2 sensor; however, it was prone to electrical noise (Figure 3) and also exhibited a higher drift.

Table 4 and Figure 4 summarize the sensitivities to KCl observed for the sensors. The sensitivities to KCl were much higher than the expected 10 mV/pKCl, based on estimations using the data presented in Section 4.1. The change in potential observed as the KCl concentration increases can be attributed to both the working and reference electrodes. Firstly, RuO_2 is known to respond to changes in ionic strength [5]. Secondly, a liquid junction potential could form at the reference electrodes due to the slow migration of compounds (impurities) in the various junctions. Lastly, the test solutions were un-buffered and some change in pH could occur during the addition of KCl. Based on this data, the RuO_2-SiO_2-based sensor displayed the best performance, in terms of acceptable sensitivity, low hysteresis, and low drift, compared to the other pH sensors.

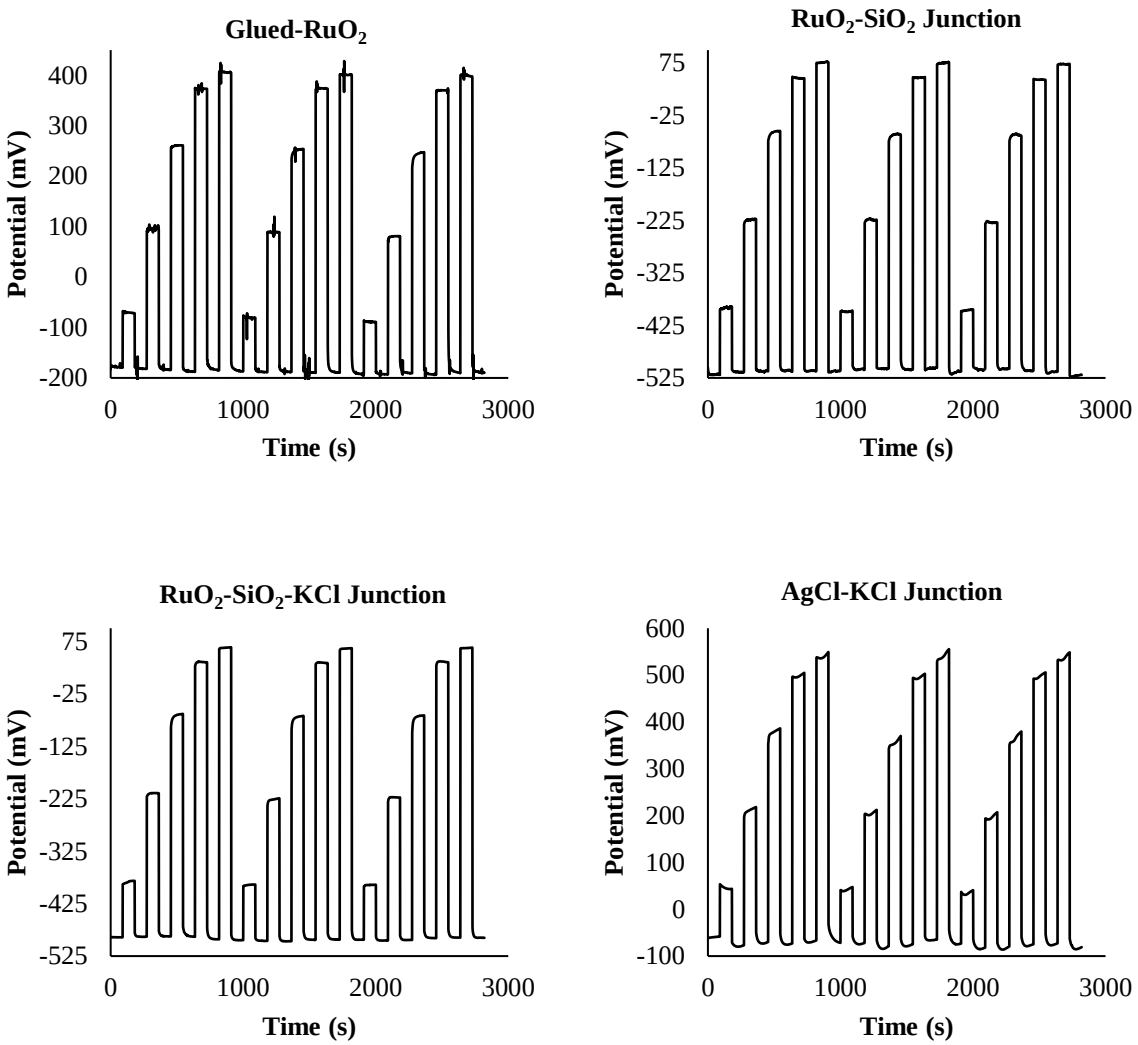

Figure 3 – pH 12–10–7–4–2–1 data loops, with pH 12 between each measurement, for RuO_2 pH sensors with Glued-RuO_2, RuO_2-SiO_2, RuO_2-SiO_2-KCl, and AgCl-KCl reference electrodes.

Table 4. Summary of KCl sensitivity values for RuO_2 pH sensors with RuO_2-SiO_2, RuO_2-SiO_2-KCl, Glued-RuO_2, and AgCl-KCl reference electrodes.

Reference Electrode	Sensitivity (mV/pKCl)		E^0		R^2
Glued-RuO_2	−16.2	±4.9	92.4	±21	0.93
RuO_2-SiO_2	−25.8	±0.8	−156	±6.2	0.99
RuO_2-SiO_2-KCl	−20.2	±2.1	−242	±14	0.93
AgCl-KCl	−31.8	±0.3	323	±2.7	0.98

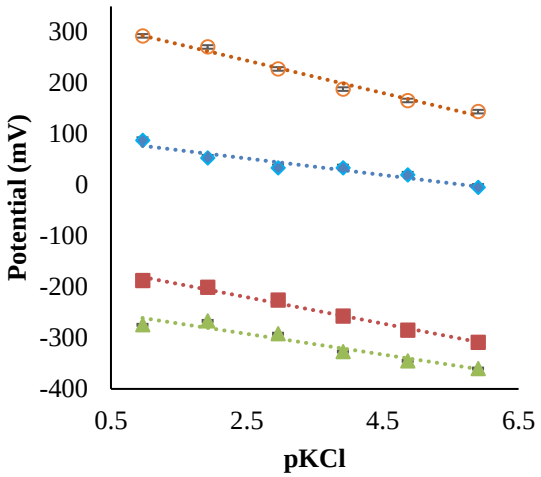

Figure 4 – KCl sensitivity of RuO_2 pH sensors with, RuO_2-SiO_2 (Red Squares), RuO_2-SiO_2-KCl (Green Triangles), Glued-RuO_2 (Aqua Diamonds), and AgCl-KCl (Orange Circles) reference electrodes.

4.5.3 Sample Solution Analysis

All developed pH sensors were evaluated in several sample matrices, including a 10 g/L solution of household borax (Borax), water sampled from a local lake (Lake), water sampled from the local beach (Sea), a common brand of cola (Cola), household vinegar (Vinegar), gastric dissolution media without enzyme (Gastric) (from Sigma), a pasteurized orange fruit drink (OJ), and a local lager beer (Beer). The samples were de-gassed where needed and allowed to equilibrate at room temperature before measurement.

Table 5 shows the pH values measured by a commercial glass pH sensor (Eetech pH700, Thermo Scientific, Singapore), which were used as the "true" value for comparison with the data collected from the different pH sensors. The average difference (error) between the "true" and measured values was calculated for each sensor. As mentioned earlier, the RuO_2-Glued sensor exhibited large shifts in potential and instability in many of the samples, resulting in poor performance. The RuO_2-SiO_2-KCl sensor returned acceptable results for most of the samples; however, the readings for the water and vinegar samples showed significant errors. The RuO_2-SiO_2 and AgCl-KCl sensor showed similar results with an average difference of 0.23 and 0.25 pH units form the glass senor, respectively. These results are presented graphically in Figure 5 as a Bland Altman plot, where the red line denotes an error of 0.5 pH units. Additionally, Figure 5 displays results obtained by the differential pH sensor developed by J. Noh et al. [25]; it is clear that the RuO_2-SiO_2 sensor developed here outperforms the differential pH sensor developed by J. Noh et al. [25].

It should be noted that the analysis of certain samples, such as white wine and fresh citrus juice, was not feasible. This was due to the presence of ascorbic acid and other redox active compounds in these

samples, such as preservatives. These types of compounds caused large shifts in potential due to the oxidization/reduction of the working electrode [7]. The results shown in Table 5 and Figure 5 demonstrate that a differential pH sensor based on a RuO_2 working electrode and a RuO_2 reference electrode with a SiO_2-loaded PVB junction can function as a reliable pH sensor in certain sample matrices.

Table 5 – Summary of pH measurements using the developed pH sensors and comparison to a commercial glass pH sensor.

Sensor	Borax	Lake	Sea	Cola	Vinegar	Gastric	OJ	Beer	Average Error
Glass pH Sensor	9.1	8.2	7.9	2.6	2.6	1.5	3.2	3.9	±0.04
Glued-RuO_2	5.8	6.5	8.3	2.8	3.5	3.7	2.5	3.5	±1.2
RuO_2-SiO_2	9.2	7.7	7.9	2.8	2.8	1.9	3.0	4.0	±0.23
RuO_2-SiO_2-KCl	9.4	9.0	9.0	2.9	3.1	1.9	3.0	4.0	±0.44
AgCl-KCl	9.3	8.6	8.4	2.9	2.7	1.6	3.3	4.2	±0.25

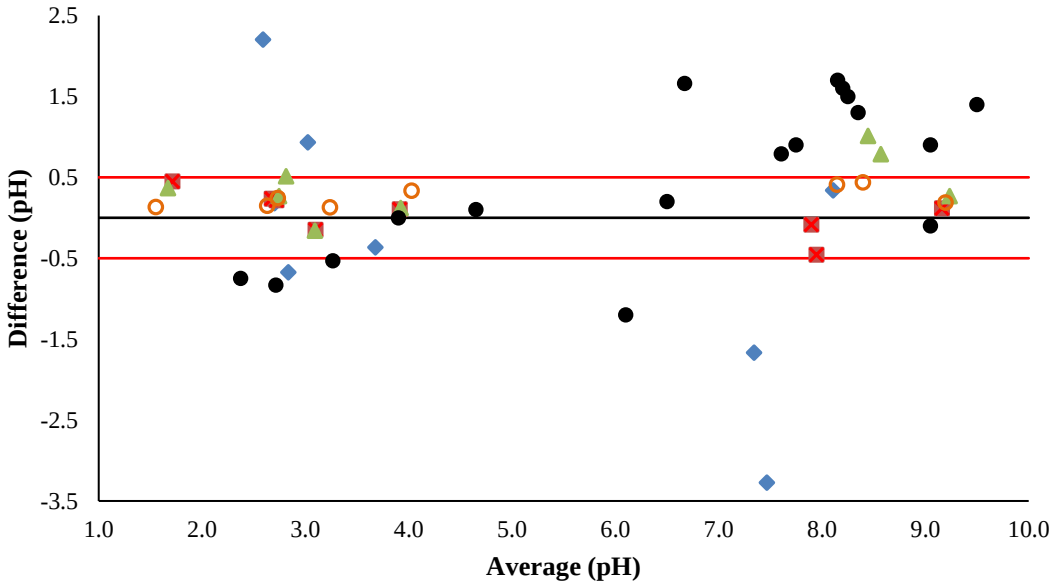

Figure 5 – Bland-Altman plot for the pH sample data for RuO_2 pH sensors with RuO_2-SiO_2 (Red Squares), RuO_2-SiO_2-KCl (Green Triangles), Glued-RuO_2 (Aqua Diamonds), and AgCl-KCl (Orange Circles) reference electrodes. Compared with sample data from the work by J. Noh et al. [25] (Black Dots). Red lines denote ±0.5 pH units from the "true" pH value.

4.6 Conclusions

A pH sensor employing a RuO_2 pH sensitive working electrode and a SiO_2-PVB junction-modified RuO_2 reference electrode has been developed and its performance evaluated. Experimental results have shown that the developed pH sensor exhibits good sensitivity (55.7 mV/pH) with low hysteresis (2.7 mV) and drift (2.2 mV/h). Experimental results have also shown that, for a selection of sample matrices, the pH values measured by the developed sensor are in excellent agreement (±0.25) with those measured by a commercial glass pH sensor. The attractive features of the developed pH sensing structure open the way towards the development of cost-effective, high-performance, and robust pH sensors for various applications.

4.7 References

1. Zhuiykov, S.; O'Brien, D.; Best, M. Water quality assessment by an integrated multi-sensor based on semiconductor RuO_2 nanostructures. *Meas. Sci. Technol.* 2009, *20*, 095201. doi:10.1088/0957-0233/20/9/095201.

2. Xu, B.; Zhang, W. Modification of vertically aligned carbon nanotubes with RuO_2 for a solid-state pH sensor. *Electrochim. Acta* 2010, *55*, 2859–2864. doi:10.1016/j.electacta.2009.12.099.

3. Manjakkal, L.; Synkiewicz, B.; Zaraska, K.; Cvejin, K.; Kulawik, J.; Szwagierczak, D. Development and characterization of miniaturized LTCC pH sensors with RuO_2 based sensing electrodes. *Sens. Actuators B Chem.* 2016, *223*, 641–649. doi:10.1016/j.snb.2015.09.135.

4. Kreider, K.G.; Tarlov, M.J.; Cline, J.P. Sputtered thin-film pH electrodes of platinum, palladium, ruthenium, and iridium oxides. *Sens. Actuators B Chem.* 1995, *28*, 167–172. doi:10.1016/0925-4005(95)01655-4.

5. Kurzweil, P. Precious metal oxides for electrochemical energy converters: Pseudocapacitance and pH dependence of redox processes. *J. Power Sources* 2009, *190*, 189–200. doi:10.1016/j.jpowsour.2008.08.033.

6. Manjakkal, L.; Cvejin, K.; Kulawik, J.; Zaraska, K.; Szwagierczak, D.; Stojanovic, G. Sensing mechanism of RuO_2–SnO_2 thick film pH sensors studied by potentiometric method and electrochemical impedance spectroscopy *J. Electroanal. Chem.* 2015, *759*, 82–90. doi:10.1016/j.jelechem.2015.10.036.

7. Lonsdale, W.; Wajrak, M.; Alameh, K. Effect of conditioning protocol, redox species and material thickness on the pH sensitivity and hysteresis of sputtered RuO_2 electrodes. *Sens. Actuators B Chem.* 2017, *252*, 251–256.

8. Maurya, D.; Sardarinejad, A.; Alameh, K. Recent Developments in R.F. Magnetron Sputtered Thin Films for pH Sensing Applications—An Overview. *Coatings* 2014, *4*, 756–771. doi:10.3390/coatings4040756.

9. Atkinson, J.K.; Glanc, M.; Prakorbjanya, M.; Sophocleous, M.; Sion, R.; Breijo, E.G. Thick film screen printed environmental and chemical sensor array reference electrodes suitable for subterranean and subaqueous deployments. *Microelectron. Int.* 2013, *30*, 92–98. doi:10.1108/13565361311314485.

10. Huang, W.-D.; Cao, H.; Deb, S.; Chiao, M.; Chiao, J.C. A flexible pH sensor based on the iridium oxide sensing film. *Sens. Actuators A Phys.* 2011, *169*, 1–11. doi:10.1016/j.sna.2011.05.016.

11. Kim, T.; Hong, S.; Yang, S. A Solid-State Thin-Film Ag/AgCl Reference Electrode Coated with Graphene Oxide and Its Use in a pH Sensor. *Sensors* 2015, *15*, 6469–6482. doi:10.3390/s150306469.

12. Kisiel, A.; Marcisz, H.; Michalska, A.; Maksymiuk, K. All-solid-state reference electrodes based on conducting polymers. *Analyst* 2005, *130*, 1655–1662. doi:10.1039/b510868c.

13. Hu, J.; Stein, A.; Bühlmann, P. Rational design of all-solid-state ion-selective electrodes and reference electrodes. *TrAC Trends Anal. Chem.* 2016, *76*, 102–114. doi:10.1016/j.trac.2015.11.004.

14. Zhang, T.; Lai, C.Z.; Fierke, M.A.; Stein, A.; Bühlmann, P. Advantages and limitations of reference electrodes with an ionic liquid junction and three-dimensionally ordered macroporous carbon as solid contact. *Anal. Chem.* 2012, *84*, 7771–7778. doi:10.1021/ac3011507.

15. Shitanda, I.; Komoda, M.; Hoshi, Y.; Itagaki, M. An instantly usable paper-based screen-printed solid-state KCl/Ag/AgCl reference electrode with long-term stability. *Analyst* 2015, *140*, 6481–6484. doi:10.1039/C5AN00617A.

16. Liao, W.; Chou, T. Fabrication of a Planar-Form Screen-Printed Solid Electrolyte Modified Ag/AgCl Reference Electrode for Application in a Potentiometric Biosensor Fabrication of a Planar-Form Screen-Printed Solid Electrolyte Modified Ag/AgCl Reference Electrode for App. *Anal. Chem.* 2006, *78*, 4219–4223. doi:10.1021/ac051562.

17. Manjakkal, L.; Zaraska, K.; Cvejin, K.; Kulawik, J.; Szwagierczak, D. Potentiometric RuO_2–Ta_2O_5 pH sensors fabricated using thick film and LTCC technologies. *Talanta* 2016, *147*, 233–240. doi:10.1016/j.talanta.2015.09.069.

18. Atkinson, J.K.; Glanc, M.; Boltryk, P.; Sophocleous, M.; Garcia-Breijo, E. An investigation into the effect of fabrication parameter variation on the characteristics of screen printed thick film silver/silver chloride reference electrodes. *Microelectron. Int.* 2011, *28*, 49–53. doi:10.1108/13565361111127368.

19. Pedrotti, J.J.; Angnes, L.; Gutz, I.G.R. Miniaturized Reference Electrodes with Microporous Polymer Junctions. *Electroanalysis* 1996, *8*, 673–675.

20. Kinlen, P.J.; Heider, J.E.; Hubbard, D.E. A solid-state pH sensor based on a Nafion-coated iridium oxide indicator electrode and a polymer-based silver chloride reference electrode. *Sens. Actuators B Chem.* 1994, *22*, 13–25. doi:10.1016/0925-4005(94)01254-7.

21. Shitanda, I.; Kiryu, H.; Itagaki, M. Improvement in the long-term stability of screen-printed planar type solid-state Ag/AgCl reference electrode by introducing poly(dimethylsiloxane) liquid junction. *Electrochim. Acta* 2011, *58*, 528–531. doi:10.1016/j.electacta.2011.09.086.

22. Guth, U.; Gerlach, F.; Decker, M.; Oelßner, W.; Vonau, W. Solid-state reference electrodes for potentiometric sensors. *J. Solid State Electrochem.* 2009, *13*, 27–39. doi:10.1007/s10008-008-0574-7.

23. Kurzweil, P. Metal Oxides and Ion-Exchanging Surfaces as pH Sensors in Liquids: State-of-the-Art and Outlook. *Sensors* 2009, *9*, 4955–4985. doi:10.3390/s90604955.

24. Blaz, T.; Migdalski, J. A. Lewenstam, Junction-less reference electrode for potentiometric measurements obtained by buffering pH in a conducting polymer matrix. *Analyst* 2005, *130*, 637–643. doi:10.1039/b418384c.

25. Noh, J.; Park, S.; Boo, H.; Kim, H.C.; Chung, T.D. Nanoporous platinum solid-state reference electrode with layer-by-layer polyelectrolyte junction for pH sensing chip. *Lab Chip* 2011, *11*, 664–671. doi:10.1039/c0lc00293c.

26. Tombcz, E. pH-dependent surface charging of metal oxides. *Period. Polytech. Chem. Eng.* 2009, *53*, 77–86. doi:10.3311/pp.ch.2009-2.08.

27. Guinovart, T.; Crespo, G.A.; Rius, F.X.; Andrade, F.J. A reference electrode based on polyvinyl butyral (PVB) polymer for decentralized chemical measurements. *Anal. Chim. Acta* 2014, *821*, 72–80. doi:10.1016/j.aca.2014.02.028.

28. Guinovart, T.; Bandodkar, A.J.; Windmiller, J.R.; Andrade, F.J.; Wang, J. A potentiometric tattoo sensor for monitoring ammonium in sweat. *Analyst* 2013, *138*, 7031–7038.

doi:10.1039/c3an01672b.

29. Guinovart, T.; Valdés-Ramírez, G.; Windmiller, J.R.; Andrade, F.J.; Wang, J. Bandage-Based Wearable Potentiometric Sensor for Monitoring Wound pH. *Electroanalysis* 2014, *26*, 1345–1353. doi:10.1002/elan.201300558.

30. Lonsdale, W.; Maurya, D.K.; Wajrak, M.; Alameh, K. Effect of ordered mesoporous carbon contact layer on the sensing performance of sputtered RuO_2 thin film pH sensor. *Talanta* 2017, *164*, 52–56. doi:10.1016/j.talanta.2016.11.020.

Chapter 5 – Development of all-RuO_2 pH sensitive electrode and modification with Ta_2O_5 and Nafion for minimisation of redox interference

This chapter is not published as an article in a journal. It is intended that the results reported here in Section 5.4.1 will be published as a journal article, once additional work is completed. Whilst, the results from Section 5.4.2 are summarised in the journal Talanta, 2018, vol. 180, pp 277-281, which is included in this thesis as Chapter 6 (Section 6.4.1). This chapter is presented in a format similar to previous chapters to maintain the consistency of this thesis.

5.1 Abstract

The following chapter bridges the published work conducted in Chapters 2, 3 and 4, with the published work conducted in Chapter 6. Briefly, a new RuO_2 pH sensitive electrode was manufactured entirely from sputter deposited RuO_2. This electrode out-performed the previously reported electrode. Additionally, the effects of redox interference were re-examined using this new electrode and their effects were minimised using Nafion and Ta_2O_5 protective layers. The results from this Chapter were then used to construct a pH sensor, which is reported in Chapter 6.

5.2 Background

In Chapters 2, 3 and 4 a pH sensor was developed, which employs sputter deposited RuO_2 on a carbon substrate. The use of an electrical contact (substrate material) was necessary since sputter deposited RuO_2 films exhibited poor durability on their own. The sputter deposition parameters used were an 8/2 Ar/O_2 ratio with 1 mTorr chamber pressure. These parameters were used since, as reported by Sardarinejad *et al.* [1], this was shown to offer higher sensitivity and lower hysteresis.

Here, however, RuO_2 was deposited using a 1/9 Ar/O_2 gas ratio at 4 mTorr chamber pressure. These RuO_2 films exhibited a more uniform appearance and adhered better to Al_2O_3 substrates, making them more durable. The reason for this improvement in durability was not investigated. Variation of sputter deposition parameters is known to alter the properties of the material produced. For example reports by K. Okimura [2] and P. Zeman [3] show that the crystal phase for sputter deposited TiO_2 changes from rutile to anatase as total sputter gas pressure increases, whilst gas composition ($Ar:O_2$ ratio) determines the deposition of metal (Ti) or oxide (TiO_2).

Increased durability of the RuO_2 film made it possible to manufacture electrodes consisting entirely of RuO_2, i.e. the working area, electrical track and electrical connection pad could all be made from RuO_2. Typically, sputter deposited metal oxide pH sensitive electrodes are deposited on an electrical substrate material, e.g. Pt, Au, Ag, and carbon. However, this creates an issue as one cannot ensure

whether the properties of the electrode being measured are due entirely to the pH sensitive metal oxide, or to a combination of the metal oxide and substrate material. For example several authors report sub-Nernstian sensitivities for their RuO_2 electrodes [4–6], which could be due to a pH dependent redox couple formed due to contaminants in their electrode or from the substrate material. Additionally, some have reported decreases in pH sensitivity for RuO_2 electrodes over time, known as ageing effects [4,7]. However, degradation or damage of the RuO_2 material on the electrode's surface could expose the substrate material (the risk of which would increase over time), resulting in a mixed potential being measured.

In this chapter, a new RuO_2 pH sensitive electrode is manufactured consisting entirely of sputter deposited RuO_2 and its sensing properties tested. Additionally, the effect of redox interference is investigated and its minimisation using Ta_2O_5 and Nafion protective layers is investigated.

5.3 Method

5.3.1 *Electrode Fabrication*

The pH sensitive working electrodes were manufactured by depositing 500 nm of RuO_2 onto a 1 mm thick Al_2O_3 substrate. RuO_2 was deposited using radio frequency magnetron sputtering (RFMS) from an RuO_2 target (99.95% purity) using 100 W sputter power with a 1:9 $Ar:O_2$ process gas ratio at 4 mTorr chamber pressure at room temperature. The electrode working area, conductive track and electrical connection-pad were formed by etching RuO_2 with a Speedy 360 Flex Trotech laser cutter/engraver (75% power, 8% speed and 4 passes). The electrode working area was isolated using Gwent dielectric paste (dried at 120 °C for 20 min), as shown in Figure 1.

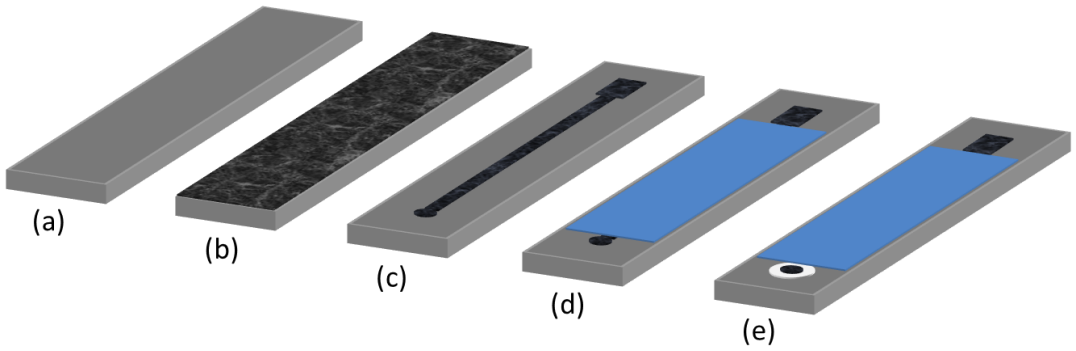

Figure 1 – Manufacture of working electrodes; (*a*) Al_2O_3 substrate, (*b*) 500 nm RuO_2, (*c)* laser etch pattern, (*d*) electrical isolation with resin, and (*e*) working area modification when required.

5.3.2 Electrode Modification

The developed RuO_2 electrodes were then modified with either 150 or 500 nm of Ta_2O_5. Ta_2O_5 was deposited using RFMS from a Ta_2O_5 target (99.95% purity) using 200 W sputter power with a 1:9 $Ar:O_2$ process gas ratio at 4 mTorr chamber pressure and room temperature. Electrodes were also modified with either a "thinner" or "thicker" coating of Nafion. "Thinner" coatings of Nafion were prepared by dip-coating electrodes by hand, 3 times, with a 5% Nafion solution (Sigma). "Thicker" layers of Nafion were prepared by drop casting 50 µL of Nafion solution onto the electrode working area. Nafion modified electrodes were cured at 230 °C for 15 min under vacuum (<10 mTorr), using rapid thermal annealing (RTA). This resulted in eight different modifications and control electrodes as per Table 1.

Table 1 - codes and structures of the different manufactured RuO_2 electrodes.

Code	Electrode
R	500 nm RuO_2
R + t	500 nm RuO_2 + 150 nm Ta_2O_5
R + T	500 nm RuO_2 + 500 nm Ta_2O_5
R + n	500 nm RuO_2 + Dip Coated Nafion
R + t + n	500 nm RuO_2 + 150 nm Ta_2O_5 + Dip Coated Nafion
R + T + n	500 nm RuO_2 + 500 nm Ta_2O_5 + Dip Coated Nafion
R + N	500 nm RuO_2 + 50 µL Nafion
R + t + N	500 nm RuO_2 + 150 nm Ta_2O_5 + 50 µL Nafion
R + T + N	500 nm RuO_2 + 500 nm Ta_2O_5 + 50 µL Nafion

5.3.3 Electrode Characterisation

An Agilent 34410A high performance digital multimeter was used to record potential between the manufactured working and reference electrodes. Potential was recorded for 180 s or 300 s at 1 s intervals using an NPLC (set to 1) operating in the high-impedance mode. Calculations were made by averaging the last 30 data points from each potential recording to produce individual measurements. These measurements were then used to calculate the sensitivity, E^*, hysteresis and drift of the sensor. Hysteresis was calculated using the difference between consecutive measurements at pH 4, whilst electrode drift was calculated using the slope of the line-of-best-fit for the data at pH 7, over the measurement period. Electrode reaction time was defined as the time taken to reach within 3 mV (i.e. 0.05 pH) of the stable potential. Measurements were made at 22 °C and error-bars represent the 95 % confidence interval. Buffer solutions were made in commercial buffer standards (Rowe Scientific) or

by adjusting Britton-Robinson buffer (0.04 M H_3BO_3, 0.04 M CH_3COOH and 0.04 M H_3PO_4) to the desired pH using 0.1 M KOH.

5.4 Results

5.4.1 pH Sensing Performance

Prior to use, the RuO_2 electrode (R) was conditioned through boiling in deionised water for 30 minutes, then equilibrated overnight in pH 7 buffer. The pH sensing performance was then evaluated by "looping" pH from 7-2-7-12 three times followed by 7-4-7-10-7 once, as shown in Figure 2. The electrode was then kept in pH 7 buffer and the test repeated after 2 and 4 months of storage. After 4 months the electrode was also accessed in buffer solutions containing 1 mM of ascorbic acid, then 1 mM of $KMnO_4$, Table 2 summarises these results.

The developed RuO_2 electrode (R) exhibited excellent performance; i.e. Nernstian sensitivity (58.8 mV/pH), linear response from pH 2 to 12 (R^2>0.9999), low hysteresis (1.3 mV), low drift (2.9 mV/h) and acceptable reaction times (<30 s), as shown in Table 2. These performance values were obtained at pH 7 equilibration and are better than the electrode reported in Chapter 3, which had to be equilibrated at pH 12, in order to obtain similar performance. When the expected mV value is subtracted from the measured mV value, a similar trend is observed for the hysteresis of the electrode (Figure 2). The pH 7 value is lower after acid exposure and higher after base exposure, however, the effects are not as pronounced, as in Chapter 3. Additionally, this electrode shows minimal change in performance when equilibrated at pH 2 or pH 12, or when aged up to 4 months. This indicates that the carbon substrate material contributed significantly to the previous electrode's performance (Chapter 3). Since, in this case, there was no substrate material, any effects can be attributed entirely to RuO_2, making this electrode superior for studying the pH and redox sensing properties of RuO_2.

Table 2 – summarises the pH sensing properties of an "all"-RuO_2 electrode, aged for up to 4 months, equilibrated at pH 7, 2 and 12, and when exposed to ascorbic acid (Asc) and MnO_4^-.

Equ.	Age (moths)	Sensitivity (mV/pH)		E^0 (mV)		R^2	Hysteresis (mV)		Drift (mV/h)
pH 7	0	-58.8	±0.5	636	±4.0	0.9999	1.3	±0.5	2.9
pH 7	2	-58.4	±0.5	602	±5.1	0.9999	0.8	±0.4	2
pH 7	4	-57.4	±0.1	626	±1.7	0.9999	4.4	±0.6	2.2
pH 2	4	-56.9	±0.4	619	±4.9	1.0000	1.6	±0.6	13
pH 12	4	-56.7	±1.2	617	±3.6	0.9997	1.6	±0.6	9.6
Asc	4	-56.8	±0.6	355	±2.3	1.0000	16	±1.0	20
MnO_4^-	4	-57.5	±2.6	911	±26	1.0000	15	±7.2	135

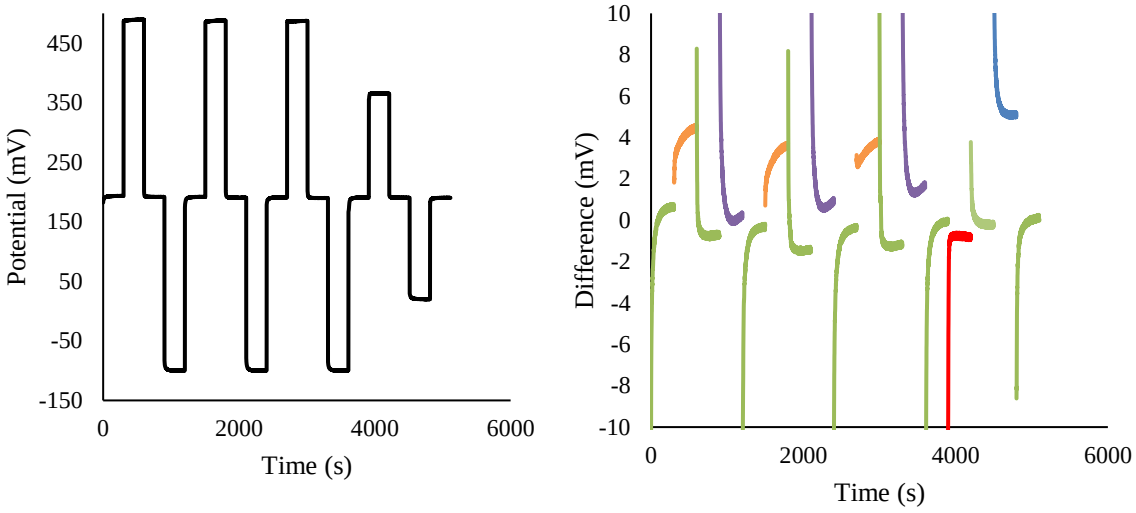

Figure 2 – Data loop from pH 7-2-7-12 three times followed by 7-4-7-10-7 once for an "all"-RuO_2 electrode (left). Right figure shows the difference between the measured potential and the expected mV value based on the line-of-best-fit for the data.

The effects of redox agents were examined on the RuO_2 electrode. Here, buffer solutions were spiked with 1 mM of ascorbic acid or MnO_4^-. The electrode was then equilibrated at pH 7 (with redox agent) for 15 minutes, before the pH was looped from 7-2-7-12 three times, shown in Figure 3. When pH measurements were performed in buffer solutions with redox agents present there was a high degree of instability observed (Figure 3), however, the drift was very repeatable. As can be seen when ascorbic acid is present, the pH 2 reading shifted negatively, while the pH 12 reading shifted positively and there was a corresponding shift in the pH 7 reading. This can be linked to the properties of ascorbic acid, which exhibits more stability in acidic solution, so it persists longer than in basic solution, where it is very unstable [8], i.e. the electrode is being reduced in the acidic solution, and re-equilibrating to a less-reduced state in the pH 12 solution. On the other hand, the opposite occurs when MnO_4^- is present since it is rapidly reduced to Mn^{2+} in acidic solutions.

This behaviour corresponds to a shift in the E^0 value, whilst the pH sensitivity remains constant, which can be confirmed by careful analysis of these data-loops. For each of the pH measurements the potential rapidly shifted and equilibrated within 30 s when exposed to a new test solution, then the measured potential began to drift. Assuming this drift is due to a shift in E^0, not sensitivity, the difference between the final reading from the previous measurement and the 30 s equilibrated value can be used to determine the pH sensing properties of the electrode (as shown in Table 2). When this analysis was performed, it reveals a Nernstian pH response, indicating that the shift in potential is indeed due to a change in E* value, as evidenced form Figure 4.

This behaviour was briefly mentioned by Fog and Buck [9], who stated that RuO_2 maintains a nearly Nernstian slope over part of the pH scale whilst the pH response of other metal oxides (IrO_2) was not reproducible in the presence of redox agents. However, here it can be seen that RuO_2 maintains a Nernstian response from pH 2 to 12 and, the E* value of a RuO_2 electrode shifts depending on its oxidisation state (i.e. the ratio of Ru^{III} to Ru^{IV} present). These results also suggest that the magnitude of this E^0 shift can be accounted for by the Nernst equation. As, mentioned in Chapter 3 if an RuO_2 electrode were to be highly oxidised or reduced, a potential shift of ± 300 mV would theoretically be expected, which is consistent with the observation here of - 262 mV when reduced and +294 mV when oxidised. This suggests the activities of Ru^{III} and Ru^{IV} at the surface of the electrode contribute to the electrode's potential. However, a potential shift due to a change in the phase boundary between the bulk/solid RuO_2 electrode and the liquid phase could also be responsible for this shift.

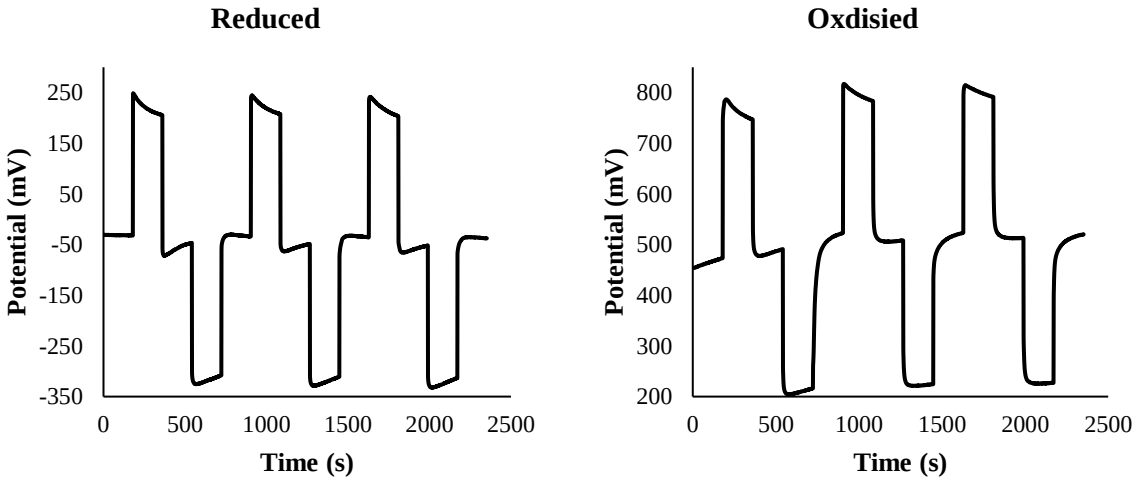

Figure 3 – Data loops from pH 7-2-7-12- three times for the RuO_2 electrode, in the presence of 1 mM ascorbic acid (left) and 1 mM MnO4- (right).

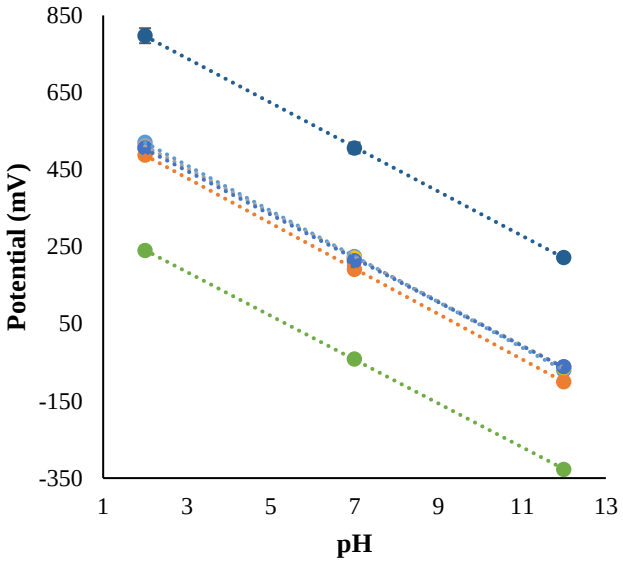

Figure 4 – Calibration plot for the RuO_2 electrode, aged for up to 4 months, equilibrated at pH 7, 2 and 12, and when exposed to ascorbic acid and MnO_4^-.

5.4.2 Electrode Modification with Ta_2O_5 and Nafion

Based on the finding from the Section 3.1, RuO_2 electrodes can only be used as pH sensors if the sample solution is free from strong redox agents, otherwise larger shift in potential will occur. To attenuate this, RuO_2 electrodes were modified with Nafion and Ta_2O_5, as per Table 1. Electrodes were conditioned as per the previous section, but the pH loop test was conducted using 5 min test intervals.

The addition of 150 or 500 nm of Ta_2O_5 (R+t and R+T, respectively) did not negatively impact the sensor, all performance-values were similar and reaction times did not increase significantly, which is consistent with the findings reported by Kou *et al*. [10] (Table 3). However, the addition of Nafion did alter the pH sensing performance of the RuO_2 electrode.

"Thinner" layers of Nafion (electrodes with 'n' in the code in Table 1) improved the sensor drift and hysteresis (Table 3), but resulted in a noticeable increase in reaction time at neutral and basic pH values, from approximately 30-60 s to 150-200s (Figure 5), which is due to slow proton transfer through the material at higher pH and is consistent with the findings of Kinlen *et al*. [11]. "Thicker" layers of Nafion (electrodes with 'N' in the code in Table 1) significantly increased the reaction time at pH 7, 10 and 12, as shown in Figure 5. However, it should be noted that the actual reaction times for these electrodes was approximately 2 - 3 hours. This can also be seen in Figure 6, where it is clear that the R+N electrode does not reach equilibration within the 5 minute test intervals. Therefore the linearity and E* results shown in Table 3 for the "thicker" Nafion electrodes was calculated without pH 10 and 12 values (the average pH 7 value was still acceptable). The calculated hysteresis for these

electrodes was also very large, however, this was due to the electrodes not fully equilibrating during the measurement period.

Table 3 – Summary of electrode performance. Note that results marked "*" were calculated without pH 10 or 12 values.

Code	Sensitivity (mV/pH)		E*		R^2	Hysteresis (mV)		Drift (mV/h)
R	-58.8	±0.47	636	±4.0	0.9999	1.3	±0.5	2.9
R + t	-58.9	±0.86	670	±3.3	0.9995	1.8	±1.2	2.8
R + T	-58.3	±0.91	669	±11	0.9997	1.8	±1.1	8.2
R + n	-57.9	±0.49	606	±4.1	0.9998	0.54	±0.47	0.48
R + t + n	-58.5	±0.54	658	±1.1	0.9998	0.57	±0.29	0.92
R + T + n	-58.6	±1.1	744	±7	0.9994	3	±1.5	0.35
R + N	-58.7	±8.5*	609	±10.6*	0.9995	31.6	±4.8	2.4
R + t + N	-56.6	±0.89*	661	±5.1*	0.9971	56.1	±9.4	15
R + T + N	-59.5	±2.8*	677	±1.4*	0.9998	46.2	±8.7	5.2

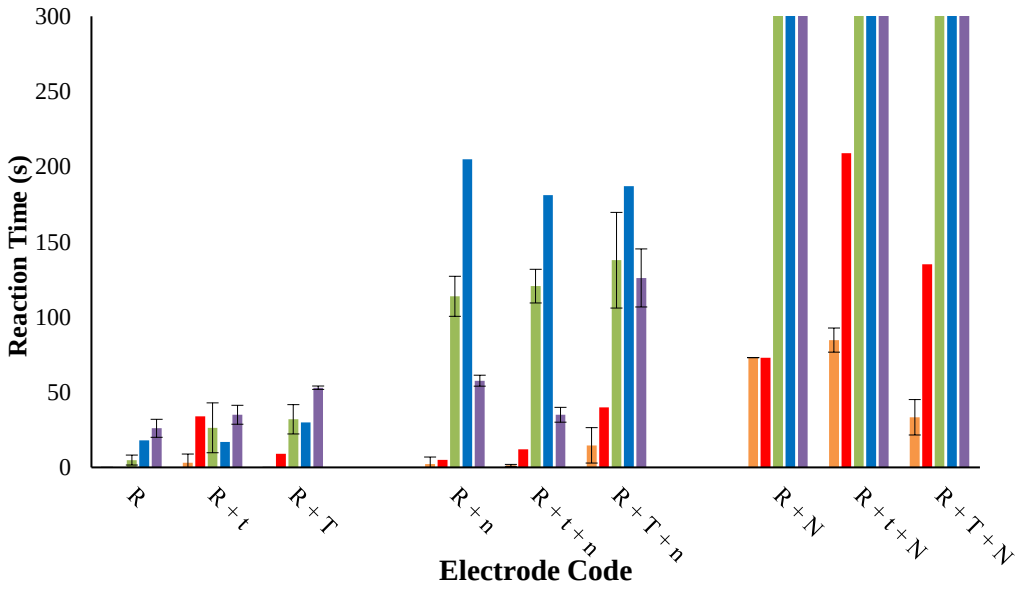

Figure 5 – Reaction times for the developed electrodes at pH 2 (orange), 4 (red), 7 (green), 10 (blue) and 12 (purple). Note that, bars that reach 300 s are actually much greater than this, in the order of several hours.

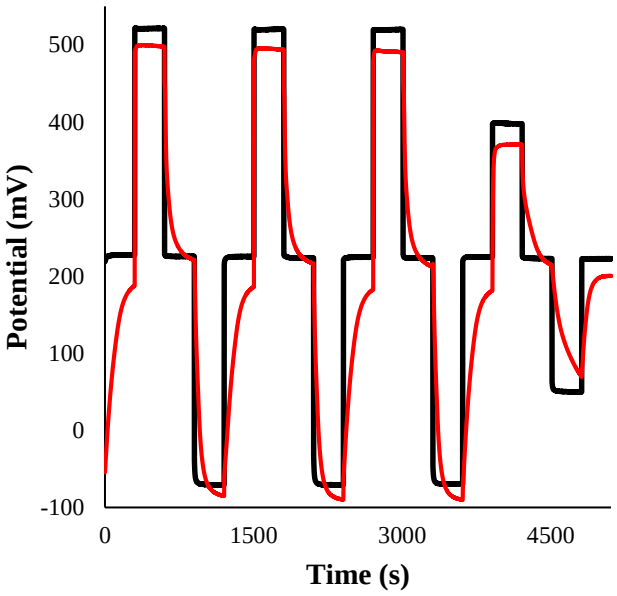

Figure 6 – 500 nm RuO_2 (Black) and 500 nm RuO_2 + 50 µL Nafion (Red) electrodes from pH 7-2-7-12 three times, followed by pH 7-4-7-10-7.

Figure 7 shows the shift in potential (interference) that occurred between a temperature controlled pH 4 buffer saturated with constant bubbling of N_2 gas for 2 hours and after 2 hours when bubbled with O_2 gas, whilst Figure 8 shows the shift in potential that occurred over 5 min when 1 mM of ascorbic acid or 1 mM of $KMnO_4$ was added to a pH 4 buffer.

As expected the unmodified RuO_2 electrode (R) showed large shifts toward all three of the redox species (Figures 7 and 8). The Ta_2O_5 modification was able to eliminate redox shifts caused by dissolved oxygen, and this is in agreement with Kou *et al.*'s [10] findings that a layer of electrically isolating Ta_2O_5 is able to block electrons generated by oxygen but still allows pH sensitivity due to proton-electron double injection. As shown in Figure 7, electrodes R+t and R+T exhibited potential shifts less than the drift reported in Section 3.1. However, Ta_2O_5 did not mitigate interference caused by stronger redox-agents such as ascorbic acid and $KMnO_4$, as evident from the large shifts shown in Figure 8. Nafion reduced the potential shift caused by dissolved oxygen, but did not completely mitigate it (Figure 7, R+n and R+N), which also suggests that Nafion is ineffective at blocking interference from neutral or cationic species due to its cation conducting nature. Nafion also reduced the interference caused by ascorbic acid and $KMnO_4$, with the "thicker" layers proving more protection than the "thinner" layers, which is in agreement with Kinlen *et al.*'s [11] findings. This behaviour can be attributed to the nature of Nafion, which when hydrated forms negatively terminated channels that are highly conductive to cations, however larger channels could permit the slow migration of non-cationic species [11].

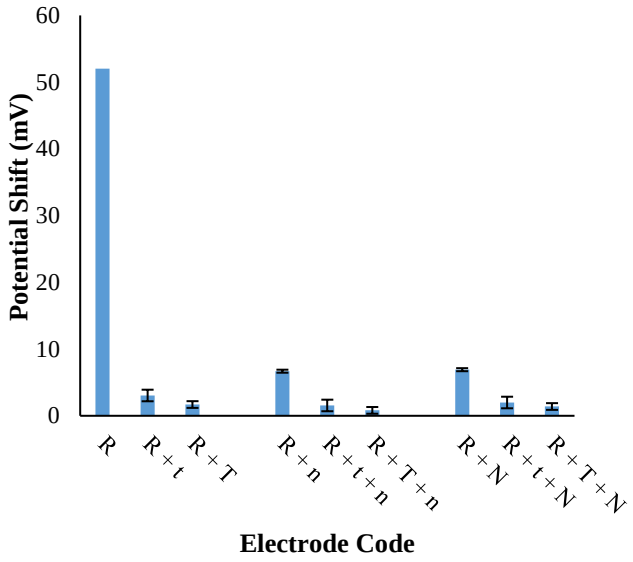

Figure 7 – Potential shift after 2 hours in oxygen saturated pH 4 buffer.

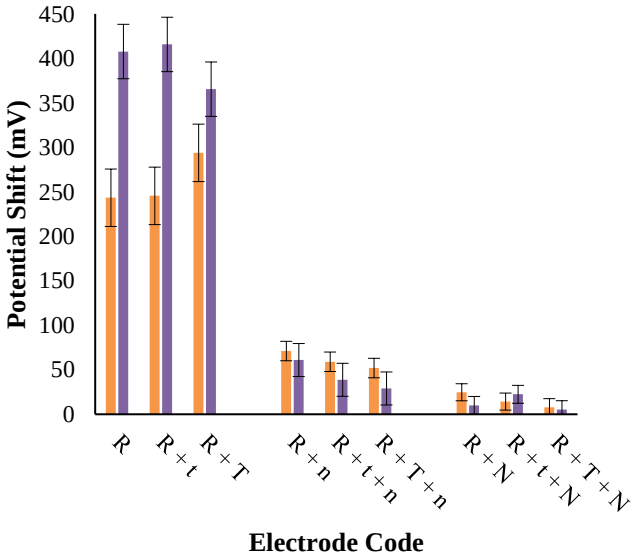

Figure 8 – Potential shift after 5 min at pH 4 caused by the redox interference from 1 mM ascorbic acid (orange) and 1 mM $KMnO_4$ (purple) for each of the electrodes.

5.5 Conclusion

RuO_2 pH sensitive electrodes without a carbon substrate material have been constructed, resulting in electrodes with superior pH sensing properties. Experimental results have shown that electrodes manufactured entirely of RuO_2 exhibit excellent performance; i.e. Nernstian sensitivity (58.8 mV/pH), linear response from pH 2 to 12 (R^2>0.9999), low hysteresis (1.3 mV), low drift (2.9 mV/h) and acceptable reaction times (<30 s). Additionally, results have shown that this electrode exhibits similar performance when equilibrated at acidic, neutral or basic pH and when aged up to 4 months.

Results also show that RuO_2 pH sensitive electrodes exhibit a shift in E* value when exposed to redox agents, but maintain a Nernstian pH response. Modification of RuO_2 electrodes with a thin layer of Ta_2O_5 (150 nm) eliminates interference from dissolved oxygen. Whilst modification with a thin layer of Nafion reduces interference from redox agents, however, increases reaction times at neutral and basic pH values. Results suggest that a RuO_2 electrode modified with a thin layer of Ta_2O_5 and a thin layer of Nafion could be more suitable for application to certain sample matrices, with "intermediate" levels of redox interfering compounds.

5.6 References

[1] A. Sardarinejad, D. Maurya, K. Alameh, The pH Sensing Properties of RF Sputtered RuO_2 Thin-Film Prepared Using Different Ar/O_2 Flow Ratio, Materials (Basel). 8 (2015) 3352–3363. doi:10.3390/ma8063352.

[2] K. Okimura, A. Shibata, N. Maeda, K. Tachibana, K. Tsuchida, Preperation of rutile TiO_2 films by RF magnetron sputtering, Jpn. J. Appl. Phys. 34 (1995) 4950.

[3] P. Zeman, S. Takabayashi, Effect of total and oxygen partial pressures on structure of photocatalytic TiO_2 films sputtered on unheated substrate, Surf. Coatings Technol. 153 (2002) 93–99. doi:10.1016/S0257-8972(01)01553-5.

[4] B. Xu, W. De Zhang, Modification of vertically aligned carbon nanotubes with RuO_2 for a solid-state pH sensor, Electrochim. Acta. 55 (2010) 2859–2864. doi:10.1016/j.electacta.2009.12.099.

[5] J.A. Mihell, J.K. Atkinson, Planar thick-film pH electrodes based on ruthenium dioxide hydrate, Sensors Actuators B Chem. 48 (1998) 505–511. doi:10.1016/S0925-4005(98)00090-2.

[6] K.G. Kreider, M.J. Tarlov, J.P. Cline, Sputtered thin-film pH electrodes of platinum, palladium, ruthenium, and iridium oxides, Sensors Actuators B. Chem. 28 (1995) 167–172. doi:10.1016/0925-4005(95)01655-4.

[7] H.N. McMurray, P. Douglas, D. Abbot, Novel thick-film pH sensors based on ruthenium dioxide-glass composites, Sensors Actuators B. Chem. 28 (1995) 9–15. doi:10.1016/0925-4005(94)01536-Q.

[8] N. Primrose, J. Schorah, M. Sobala, Implications for Gastric Carcinogenesis13, Am. J. Clin. Nutr. 53 (1991) 287S–93S.

[9] A. Fog, R.P. Buck, Electronic semiconducting oxides as pH sensors, Sensors and Actuators. 5

(1984) 137–146. doi:10.1016/0250-6874(84)80004-9.

[10] L.M. Kuo, Y.C. Chou, K.N. Chen, C.C. Lu, S. Chao, A precise pH microsensor using RF-sputtering IrO_2 and Ta_2O_5 films on Pt-electrode, Sensors Actuators, B Chem. 193 (2014) 687–691. doi:10.1016/j.snb.2013.11.109.

[11] P.J. Kinlen, J.E. Heider, D.E. Hubbard, A solid-state pH sensor based on a Nafion-coated iridium oxide indicator electrode and a polymer-based silver chloride reference electrode, Sensors Actuators B Chem. 22 (1994) 13–25. doi:10.1016/0925-4005(94)01254-7.

Chapter 6 of this thesis is currently not available in this version of the thesis.

This chapter has been published as:

W. Lonsdale, M. Wajrak, K. Alameh, Manufacture and Application of Solid-State RuO2 Metal-Oxide pH sensor to Beverages, Talanta. 180 (2018) 277-281. doi:10.1016/j.talanta.2017.12.070

Chapter 7 – Conclusions and Future Work

Initially, in this project, a RuO_2 pH sensitive working electrode was develop by sputter depositing RuO_2 onto carbon substrate material (Chapters 2 and 3). RuO_2 pH sensitive electrodes manufactured by sputter deposition onto carbon substrates are not ideal. Electrodes manufactured this way suffer from slow pH dependent shifts in potential and must be equilibrated at basic pH values in order to obtain best performance. More ideal pH sensitive electrodes can be manufactured by sputter depositing only RuO_2 onto Al_2O_3 substrates (Chapter 5). Such electrodes exhibit Nernstian pH response from pH 2-12 and do not suffer from shifts in potential caused by equilibration at acidic or basic pH. Additionally, such electrodes were durable and performance did not decrease significantly over a 4 month test period.

The pH sensing properties of RuO_2 (sensitivity, hysteresis and drift), between pH 2-12, can be explained solely using the Nernst equation. The pH sensitivity of RuO_2 is Nernstian, whilst hysteresis and drift can be explained as shifts in the E* value, which is determined by the standard redox potential (E^0) and fluctuation in the Ru^{III} to Ru^{IV} ratio. Fluctuations in the Ru^{III} to Ru^{IV} ratio also explain redox interference. Redox interference from anions can be reduced, but not completely eliminated, by the addition of a Nafion layer. Thicker layers provide more protection (than thinner layers), however, they increase the reaction time of the sensor at neutral and basic pH values. A rate of 5 µL of 5% Naifon solution per 3.14 cm^2 electrode area proved useful for the analysis of some beverages, while the sensitivity to dissolved oxygen for RuO_2 electrodes can be eliminated by addition of a thin layer (80 nm) of sputter deposited Ta_2O_5 (Chapter 5).

The second phase of this project involved the development of a reference electrode. Reference electrodes can be manufacture by modifying RuO_2 working electrodes with a porous PVB junction (Chapter 4 and 6). Whilst this is not a "true" reference electrode, when equilibrated, a suitably stable potential is obtained and pH measurements can be made. Though this reference electrode required frequent calibration, since, it does not contain KCl that leaches slowly, the lifetime of the reference electrode could be considerable longer than that of reference electrodes based on Ag|AgCl|KCl.

Finally, an all solid state pH sensor was constructed by combining the working electrode developed in Chapter 5 with the reference electrode develop in Chapter 4. This pH sensor consisted entirely of (i) sputter deposited RuO_2 modified with protective layers of Ta_2O_5 and Nafion, thus minimising redox interference and (ii) a reference electrode modified with a porous PVB junction. The sensor performed well in a wider variety of sample matrices, with a precision of ± 0.08 pH units. Which based on literature review (Chapter 1) is the highest level of precision achieved (to date) for a RuO_2 based pH sensor in real samples. Though this sensor displayed excellent performance in the samples tested, it is still inferior to glass pH sensors in some ways, as it requires frequent calibration and is unable to accurately measure pH in all sample matrices, due to interference from strong redox agents.

However, the developed sensor is advantageous compared to traditional glass pH sensors, due to its solid state construction, making it mechanically robust/durable and has the potential to be miniaturised. The sensor developed here could be further developed into a hand-held or in-situ type device for pH measurements.

Based on the findings from the work conducted throughout this PhD project, improvements to the sensor could be made as follows. Firstly, a sensor could be manufactured without the Nafion protective layer. This would result in a sensor with much faster reaction times and could be used over a wider pH range (2-12, instead of 2-6). Additionally, given the pH response slope of the sensor does not change in the presence of oxidising or reducing agents, it may be possible to equilibrate the sensor to such a sample, then account for the shift in E* value by recalibration. This could potentially make RuO_2 based pH sensors more advantageous then IrO_2 based sensors, since the sensitivity of IrO_2 is suppressed in the presence of redox agents. The thickness of RuO_2 (500 nm) used was optimised on carbon substrates. Given the carbon material has been removed, this thickness may not be needed. However, since RuO_2 is being used as an electrical connection pad, a fairly robust layer of RuO_2 is still needed. In addition, the effects of temperature were not studied in this work. Since pH sensitivity depends on temperature it will be necessary to account for temperate fluctuation if a sensor is to be constructed. However, since the working and reference electrodes of this sensor are constructed form the same material, the effects of temperature on the measured potential may cancel out. Though, other factors at the porous PVB junction may influence this.

Appendix

Statement of Contribution

To Whom It May Concern,

I Wade Lonsdale, conceived, designed and undertook all experiments. Wade Lonsdale analysed all data, interpreted results and authored the publications. Prof. Kamal Alameh and Dr. Magdalena Wajrak interpreted results and edited the publications entitled:

- W. Lonsdale, D.K. Maurya, M. Wajrak, K. Alameh, Effect of ordered mesoporous carbon contact layer on the sensing performance of sputtered RuO_2 thin film pH sensor, Talanta. 164 (2017) 52–56. doi:10.1016/j.talanta.2016.11.020.

- W. Lonsdale, M. Wajrak, K. Alameh, Effect of conditioning protocol, redox species and material thickness on the pH sensitivity and hysteresis of sputtered RuO_2 electrodes, Sensors Actuators B Chem. 252 (2017) 251–256. doi:10.1016/j.snb.2017.05.171

- W. Lonsdale, M. Wajrak, K. Alameh, RuO_2 pH Sensor with Super-Glue-Inspired Reference Electrode, Sensors. 17 (2017) 2036. doi:10.3390/s17092036.

- W. Lonsdale, M. Wajrak, K. Alameh, Manufacture and Application of Solid-State RuO_2 Metal-Oxide pH sensor to Beverages, Talanta. 180 (2018) 277-281. doi:10.1016/j.talanta.2017.12.070

Wade Lonsdale

I, as a Co-Author, endorse that this level of contribution by the Candidate indicated above is appropriate.

Prof. Kamal Alameh

Electron Science Research Institute, Edith Cowan University, Joondalup, WA 6027, Australia

Dr. Magdalena Wajrak

School of Science, Edith Cowan University, Joondalup, WA 6027, Australia